

CRITICAL SURFACE OF THE 1-2 MODEL

GEOFFREY R. GRIMMETT AND ZHONGYANG LI

ABSTRACT. The 1-2 model on the hexagonal lattice is a model of statistical mechanics in which each vertex is constrained to have degree either 1 or 2. There are three types of edge, and three corresponding parameters a, b, c . It is proved that, when $a \geq b \geq c > 0$, the surface given by $\sqrt{a} = \sqrt{b} + \sqrt{c}$ is critical. The proof hinges upon a representation of the partition function in terms of that of an Ising-type model on an enhanced graph, and thereby on the partition function of a dimer model. This dimer model may be studied via the Pfaffian representation of Fisher, Kasteleyn, and Temperley. It is proved, in addition, that the two-edge correlation function decays exponentially with distance when $a^2 < b^2 + c^2$.

1. INTRODUCTION AND BACKGROUND

The 1-2 model on the hexagonal lattice was introduced by Schwartz and Bruck [24] as an intermediary in the calculation of the capacity of a constrained coding system. They expressed the capacity via holographic reductions (see [27]) in terms of the number of perfect matchings (or dimer configurations), and the latter may be studied via the Pfaffian method of Fisher, Kasteleyn, and Temperley [10, 14, 25]. The 1-2 model may be viewed as a model of statistical mechanics of independent interest, and it is related to the Ising model and the dimer model. In the current paper, we study the 1-2 model within this context, and we establish the exact form of the associated critical curve.

A 1-2 configuration on the hexagonal lattice $\mathbb{H} = (\mathbb{V}, \mathbb{E})$ is a subset F of edges such that every vertex is incident with either one or two edges of F . There are three real parameters $a, b, c > 0$, which are associated with the three classes of edges of \mathbb{H} . The weight of a configuration on a finite region is the product over vertices v of one of a, b, c chosen according to the edge-configuration at v . (See Figure 2.2.)

Through a sequence of transformations, the 1-2 model turns out to be linked to an enhanced Ising model, a polygon model, and a dimer model. These connections are pursued here, and in the linked paper [13]. The main result (Theorem 3.1) states

Date: June 27, 2015.

2010 Mathematics Subject Classification. 82B20, 60K35, 05C70.

Key words and phrases. 1-2 model, Ising model, dimer model, perfect matching, Kasteleyn matrix.

that, when $a \geq b \geq c > 0$, the surface given by $\sqrt{a} = \sqrt{b} + \sqrt{c}$ is critical. This is proved by an analysis of the behaviour of the two-edge correlation function $\langle \sigma_e \sigma_f \rangle$ as $|e - f| \rightarrow \infty$. The model is called *uniform* if $a = b = c = 1$, and thus the uniform model is not critical in the above sense.

There has been major progress in recent years in the study of two-dimensional Ising models via rhombic tilings and discrete holomorphic observables (see, for example, [5, 6, 7, 16]). There is a rhombic representation of the critical polygon model associated with the 1-2 model, and an associated discrete holomorphic function, but this is not explored here.

It was shown already in [20] that a (geometric) phase transition exists for the 1-2 model on \mathbb{H} . An *a-cluster* is a connected set of vertices each having local weight a (as above). It was shown that there exists, a.s. with respect to any translation-invariant Gibbs measure, no infinite path of present edges. In contrast, for given b, c , there exists no infinite a -cluster for small a , whereas such a cluster exists for large a . The a.s. uniqueness of infinite ‘homogeneous’ clusters was proved in [22].

This paper is concentrated on the 1-2 model and its dimer representation. A related representation involves the polygon model on \mathbb{H} , and the phase transition of the latter model is the subject of the linked paper [13]. The polygon representation is related to the high temperature expansion of the Ising model, and results in an inhomogeneous model that may be regarded as an extension of the $O(n)$ model with $n = 1$; see [9] for a recent reference to the $O(n)$ model.

The structure of the current work is as follows. The precise formulation of the 1-2 model appears in Section 2, and the main theorem (Theorem 3.1) is presented in Section 3.

The 1-2 model is coupled with an Ising model in Section 4, in a manner not dissimilar to the Edwards–Sokal coupling of the random-cluster model (see [12, Sect. 1.4]). It may be transformed into a dimer model (see [20]) as described in Section 5. In Section 6, we gather some conclusions about infinite-volume free energy and infinite-volume measures that are new for the 1-2 model. This is followed in Section 7 by the proof of exponential decay of the two-edge function, subject to the further condition of Theorem 3.2. Theorem 3.1 is proved in Section 8 via an analysis using Pfaffians.

2. THE 1-2 MODEL

Let $G = (V, E)$ be a finite graph. A *1-2 configuration* on G is a subset $F \subseteq E$ such that every $v \in V$ is incident to either one or two members of F . The subset F may be expressed as a vector in the space $\Sigma = \{-1, +1\}^E$ where -1 represents an absent edge and $+1$ a present edge. Thus the space of 1-2 configurations may be

viewed as the subset of Σ containing all vectors σ such that

$$\sum_{e \ni v} \sigma'_e \in \{1, 2\}, \quad v \in V,$$

where

$$(2.1) \quad \sigma'(e) = \frac{1}{2}(1 + \sigma(e)).$$

(In Section 4.2, we will write Σ^e for Σ , in order to distinguish it from a space of vertex-spins to be denoted Σ^v .)

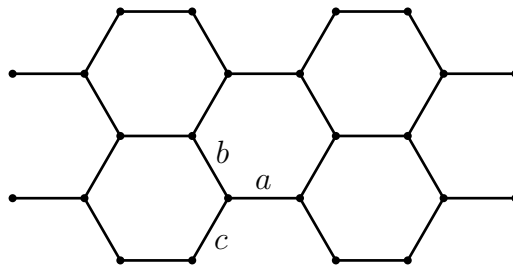


FIGURE 2.1. An embedding of the hexagonal lattice. Horizontal edges are said to be of type a , NW/SE edges of type b , and NE/SW edges of type c .

Suppose now that G is a finite part of the hexagonal lattice \mathbb{H} , suitably embedded in \mathbb{R}^2 , see Figure 2.1. The embedding is such that each edge may be viewed as one of: horizontal, NW/SE, or NE/SW. (Later we shall consider a finite box with toroidal boundary conditions.) Let $a, b, c \geq 0$ be such that $(a, b, c) \neq (0, 0, 0)$, and associate these three parameters with the edges as indicated in the figure. For $\sigma \in \Sigma$ and $v \in V$, let $\sigma|_v$ be the sub-configuration of σ on the three edges incident to v . There are $2^3 = 8$ possible local configurations, which we encode as words of length three in the alphabet with letters $\{0, 1\}$. That is, for $v \in V$, we observe the states $\sigma(e_{v,a}), \sigma(e_{v,b}), \sigma(e_{v,c})$, where $e_{v,a}, e_{v,b}, e_{v,c}$ are the edges of type a, b, c (respectively) incident to v . The corresponding *signature* s_v is the word $\sigma'(e_{v,c})\sigma'(e_{v,b})\sigma'(e_{v,a})$ of length 3, where σ' is given in (2.1). That is, the signature of v is given as in Figure 2.2, together with the local weight $w(\sigma|_v)$ associated with each of the eight possible signatures.

The hexagonal lattice \mathbb{H} is, of course, bipartite, and we colour the two vertex-classes *black* and *white*. The upper diagrams of Figure 2.2 are for black vertices, and the lower for white vertices.

To the vector $\sigma \in \Sigma$, we assign the weight

$$(2.2) \quad w(\sigma) = \prod_{v \in V} w(\sigma|_v).$$

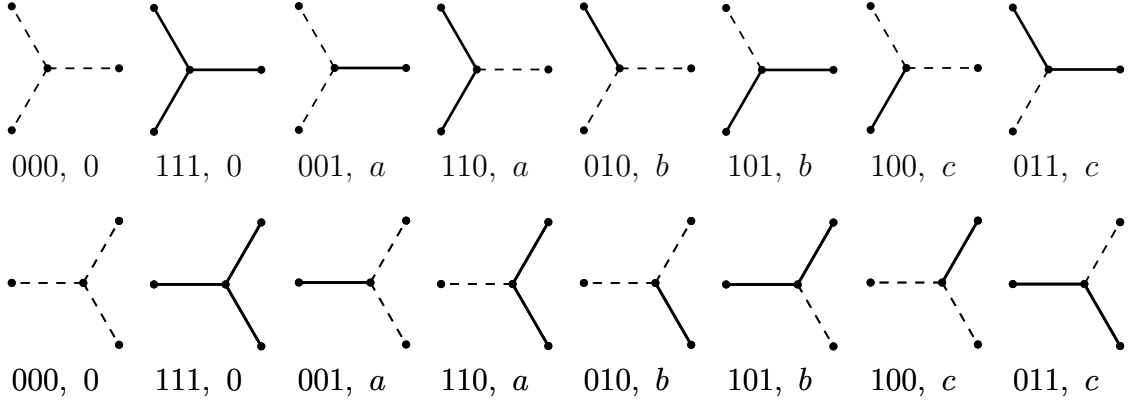


FIGURE 2.2. The eight possible local configurations $\sigma|_v$ at a vertex v in the two cases of *black* and *white* vertices. The signature of each is given, and also the local weight $w(\sigma|_v)$ associated with each instance.

These weights give rise to the partition function

$$(2.3) \quad Z = \sum_{\sigma \in \Sigma} w(\sigma),$$

which leads in turn to the probability measure

$$(2.4) \quad \mu(\sigma) = \frac{1}{Z} w(\sigma), \quad \sigma \in \Sigma.$$

It is easily seen that the measure μ is invariant under the mapping $(a, b, c) \mapsto (ka, kb, kc)$ with $k > 0$. It is therefore natural to re-parametrize the 1-2 model by

$$(2.5) \quad (a', b', c') = \frac{(a, b, c)}{\|(a, b, c)\|_2}.$$

We will work mostly with a finite subgraph of \mathbb{H} subject to toroidal boundary conditions. Let $n \geq 1$, and let τ_1, τ_2 be the two shifts of \mathbb{H} , illustrated in Figure 2.3, that map an elementary hexagon to the next hexagon in the given directions. The pair (τ_1, τ_2) generates a \mathbb{Z}^2 action on \mathbb{H} , and we write \mathbb{H}_n for the quotient graph of \mathbb{H} under the subgroup of \mathbb{Z}^2 generated by τ_1^n and τ_2^n . The resulting \mathbb{H}_n is illustrated in Figure 2.3, and may be viewed as a finite subgraph of \mathbb{H} subject to toroidal boundary conditions.

Our purpose in this paper is to study the 1-2 measure (2.4) on \mathbb{H}_n in the infinite-volume limit as $n \rightarrow \infty$, and to identify its critical surface. As an indicator of phase transition, we shall use the two-point function $\langle \sigma_e \sigma_f \rangle_n$, where e, f are two edges and $\langle \cdot \rangle_n$ denotes expectation.

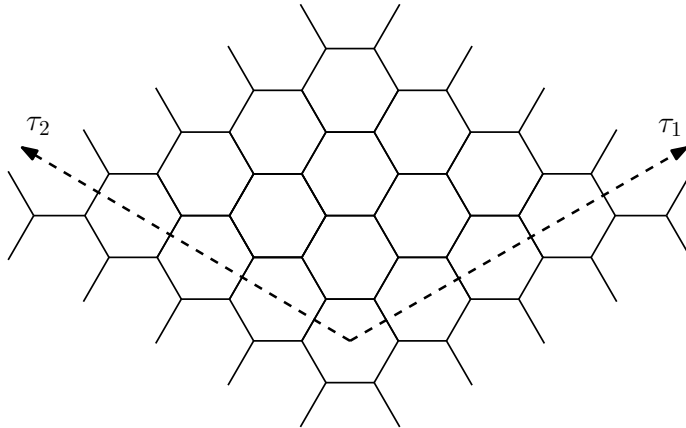


FIGURE 2.3. The graph \mathbb{H}_n is an $n \times n$ ‘diamond’ wrapped onto a torus, as illustrated here with $n = 4$.

We do not explore in detail the nature and multiplicity of infinite-volume measures in this paper. There are certain complexities in such issues arising from the absence of a correlation inequality, and some partial results along these lines may be found in [20, Thm 0.1]. These results are developed in Section 6, where the main result of current value is the existence of the infinite-volume limit of the toroidal 1-2 measure, see Theorem 6.2.

3. MAIN RESULTS

Consider the 1-2 model on \mathbb{H}_n with parameters $a, b, c > 0$. We write $e = \langle x, y \rangle$ for the edge e with endpoints x, y , and we use $\langle X \rangle_n$ to denote expectation of the random variable X with respect to the probability measure of (2.4) on \mathbb{H}_n . We shall make use of a measure of distance $|e - f|$ between e and f , and it is largely immaterial which measure we take. For definiteness, consider \mathbb{H} embedded in \mathbb{R}^2 in the manner of Figure 2.3, with unit edge-lengths, and let $|e - f|$ be the Euclidean distance between their midpoints.

Theorem 3.1. *Let $a, b, c > 0$, and let $e, f \in \mathbb{E}$ be NW/SE edges such that:*

- (3.1) *there exists a path $\pi = \pi(e, f)$ of \mathbb{H}_n from e to f using only horizontal and NW/SE half-edges.*
- (a) *The limit $\langle \sigma_e \sigma_f \rangle = \lim_{n \rightarrow \infty} \langle \sigma_e \sigma_f \rangle_n$ exists.*
 - (b) *Let $a \geq b > 0$. For almost every $c > 0$ satisfying either $\sqrt{a} > \sqrt{b} + \sqrt{c}$ or $\sqrt{c} > \sqrt{a} + \sqrt{b}$, we have that $\lim_{|e-f| \rightarrow \infty} \langle \sigma_e \sigma_f \rangle^2$ exists and is non-zero.*
 - (c) *If $a \geq b > 0$ and $\sqrt{a} - \sqrt{b} < \sqrt{c} < \sqrt{a} + \sqrt{b}$, then $\langle \sigma_e \sigma_f \rangle \rightarrow 0$ as $|e - f| \rightarrow \infty$.*

Thus, the two-edge function $\langle \sigma_e \sigma_f \rangle$ behaves in a qualitatively different manner depending on whether or not $\sqrt{a} - \sqrt{b} < \sqrt{c} < \sqrt{a} + \sqrt{b}$. Here is a motivation for condition (3.1). Consider the ‘ground states’ when either $c = 0$ or $a = b = 0$. By examination of the different cases in Figure 2.2, we may see, subject to (3.1), that

$$(3.2) \quad \langle \sigma_e \sigma_f \rangle = 1 \quad \text{if either } a, b > 0, c = 0, \quad \text{or } a = b = 0, c > 0.$$

The result of part (b) will follow from this by an argument using analyticity (and, moreover, the set of c at which the conclusion of (b) fails is a union of isolated points). The theorem remains true with e, f assumed to be horizontal rather than NW/SE.

Theorem 3.1 is not necessarily a complete picture of the location of critical phenomena of the 1-2 model, since the conditions on the parameters are allied to the direction of the vector from e to f . (The direction NW/SE is privileged in the above theorem. Similar results hold for the other two lattice directions with suitable permutations of the parameters.) We have not ruled out the possibility of further critical surfaces in the parameter-space $[0, \infty)^3$.

One may ask for the rate of decay to zero of the limit $\langle \sigma_e \sigma_f \rangle$ as $|e - f| \rightarrow \infty$, in part (c) above, and we have a partial result in this direction under a stronger condition.

Theorem 3.2. *Let $a \geq b \geq c > 0$ and assume that $a^2 < b^2 + c^2$. There exists $\alpha(a, b, c) > 0$ such that*

$$\langle \sigma_e \sigma_f \rangle \leq e^{-\alpha|e-f|}, \quad e, f \in \mathbb{E}.$$

The proofs of the above utilize a sequence of transformations between the 1-2 model and the Ising and dimer models, as described in the forthcoming sections. Theorem 3.1 is proved in Section 8, and Theorem 3.2 (in an apparently more general form) in Section 7.

4. SPIN REPRESENTATIONS OF THE 1-2 MODEL

Two spin representations of the 1-2 model are presented here. In the first, the 1-2 partition function is rewritten in terms of edge-spins. The second is reminiscent of the random-cluster representation of the Potts model. A further set of spin-variables are introduced at the vertices of the graph, together with an Ising-type partition function.

4.1. The 1-2 model as a spin system. Let $\mathbb{H}_n = (V_n, E_n)$ be the quotient hexagonal lattice embedded in the torus in the manner of Figure 2.3. Let $\Sigma = \{-1, +1\}^{E_n}$, where -1 (respectively, $+1$) represents an absent edge (respectively, present edge).

For $\sigma \in \Sigma$ and $v \in V_n$, let $\sigma_{v,a}$, $\sigma_{v,b}$, $\sigma_{v,c}$ denote the spins on the incident a -edge, b -edge, c -edge of v . Two partition functions Z, Z' generate the same measure whenever they differ only in a multiplicative factor (that is, their weight functions

satisfy $w(\sigma) = cw'(\sigma)$ for some $c \neq 0$ and all $\sigma \in \Sigma$), in which case we write $Z \doteq Z'$. We represent the 1-2 model as a spin system as follows.

Proposition 4.1. *Let $a, b, c \geq 0$ such that $(a, b, c) \neq (0, 0, 0)$. The 1-2 model with parameters a, b, c on \mathbb{H}_n has partition function Z_n satisfying $Z_n \doteq Z'_n$ where*

$$(4.1) \quad Z'_n := \sum_{\sigma \in \Sigma} \prod_{v \in V_n} (1 + A\sigma_{v,b}\sigma_{v,c} + B\sigma_{v,a}\sigma_{v,c} + C\sigma_{v,a}\sigma_{v,b}),$$

and

$$(4.2) \quad A = \frac{a - b - c}{a + b + c}, \quad B = \frac{b - a - c}{a + b + c}, \quad C = \frac{c - a - b}{a + b + c}.$$

Proof. By examination of (4.1), we see that a vertex with local configuration labelled a in Figure 2.2 has weight

$$1 + A - B - C = \frac{4a}{a + b + c},$$

with similar expressions for vertices with the other possible signatures. This is in agreement with (2.2)–(2.3), and the claim follows. \square

4.2. Coupled Ising representation. Let $A\mathbb{H}_n = (AV_n, AE_n)$ be the graph derived from $\mathbb{H}_n = (V_n, E_n)$ by adding a vertex at the midpoint of each edge in E_n . Let $ME_n = \{Me : e \in E_n\}$ be the set of such midpoints, and $AV_n = V_n \cup ME_n$. The edges AE_n are precisely the half-edges of E_n , each being of the form $\langle v, Me \rangle$ for some $v \in V_n$ and incident edge $e \in E_n$.

We introduce an Ising-type model on the graph $A\mathbb{H}_n$. The marginal of the model on midpoints ME_n is a 1-2 model, and the marginal on V_n is an Ising model. This enhanced Ising model is reminiscent of the coupling of the Potts and random-cluster measures, see [12, Sect. 1.4]. It is constructed initially via a weight function on configuration space, and via the associated partition function. The weights may be complex-valued, and thus there does not always exist an associated probability measure.

The better to distinguish between V_n and ME_n , we set $\Sigma^e = \{-1, +1\}^{ME_n}$ as before, and $\Sigma^v = \{-1, +1\}^{V_n}$. An edge $e \in E_n$ is identified with the element of ME_n at its centre. A spin-vector is a pair $(\sigma^e, \sigma^v) \in \Sigma^e \times \Sigma^v$ with $\sigma^e = (\sigma_{v,s} : v \in V_n, s = a, b, c)$ and $\sigma^v = (\sigma_v : v \in V_n)$, to which we allocate the (possibly negative, or even complex) weight

$$(4.3) \quad \prod_{v \in V_n} (1 + \epsilon_a \sigma_v \sigma_{v,a})(1 + \epsilon_b \sigma_v \sigma_{v,b})(1 + \epsilon_c \sigma_v \sigma_{v,c}),$$

where $\epsilon_a, \epsilon_b, \epsilon_c \in \mathbb{C}$ are constants associated with horizontal, NW/SE, and NE/SW edges, respectively, and $\sigma_{v,a}, \sigma_{v,b}, \sigma_{v,c}$ denote the spins on midpoints of the corresponding edges incident to $v \in V_n$. If u and v are endpoints of the same edge $\langle u, v \rangle$

of \mathbb{H}_n , then $\sigma_{u,a} = \sigma_{v,a}$. In (4.3), each factor $1 + \epsilon_s \sigma_v \sigma_{v,s}$ ($s = a, b, c$) corresponds to a half-edge of \mathbb{H}_n . Recalling that

$$(4.4) \quad e^{x\sigma_1\sigma_2} = (1 + \sigma_1\sigma_2 \tanh x) \cosh x, \quad x \in \mathbb{R}, \quad \sigma_1\sigma_2 = \pm 1,$$

the above spin system is a ferromagnetic Ising model on $A\mathbb{H}_n$ when $\epsilon_a, \epsilon_b, \epsilon_c \in (0, 1)$.

4.3. Marginal on the midpoints ME_n . The partition function of (4.3) is

$$(4.5) \quad Z_n(I) := \sum_{\sigma^e \in \Sigma^e} \sum_{\sigma^v \in \Sigma^v} \prod_{v \in V_n} (1 + \epsilon_a \sigma_v \sigma_{v,a}) (1 + \epsilon_b \sigma_v \sigma_{v,b}) (1 + \epsilon_c \sigma_v \sigma_{v,c}).$$

The product, when expanded, is a sum of monomials in which each σ_v has a power between 0 and 3. On summing over σ^v , only terms with even powers of the site-spins σ_v survive, and furthermore $\sigma_v^2 = 1$, so that

$$Z_n(I) = \sum_{\sigma^e \in \Sigma^e} \prod_{v \in V_n} (1 + \epsilon_b \epsilon_c \sigma_{v,b} \sigma_{v,c} + \epsilon_a \epsilon_c \sigma_{v,a} \sigma_{v,c} + \epsilon_a \epsilon_b \sigma_{v,a} \sigma_{v,b}).$$

Let $a, b, c > 0$ be such that $ABC \neq 0$ where A, B, C are given by (4.2), and let

$$(4.6) \quad \epsilon_a = \sqrt{\frac{BC}{A}}, \quad \epsilon_b = \sqrt{\frac{AC}{B}}, \quad \epsilon_c = \sqrt{\frac{AB}{C}}.$$

By (4.1),

$$(4.7) \quad Z_n(I) = Z'_n,$$

whence the marginal model of (4.3) on the midpoints of edges of \mathbb{H}_n , subject to (4.6), is simply the 1-2 model with parameters a, b, c .

4.4. Marginal on the vertices V_n . This time we perform the sum over σ^e in (4.5). Let $g = \langle u, v \rangle \in E_n$ be an edge with weight ϵ_g . We have

$$(4.8) \quad \sum_{\sigma_g = \pm 1} (1 + \epsilon_g \sigma_u \sigma_g) (1 + \epsilon_g \sigma_v \sigma_g) = 2 (1 + \epsilon_g^2 \sigma_u \sigma_v),$$

$$(4.9) \quad \sum_{\sigma_g = \pm 1} \sigma_g (1 + \epsilon_g \sigma_u \sigma_g) (1 + \epsilon_g \sigma_v \sigma_g) = 2\epsilon_g (\sigma_u + \sigma_v).$$

By (4.5) and (4.8),

$$(4.10) \quad Z_n(I) = 2^{|E_n|} \sum_{\sigma^v \in \Sigma^v} \prod_{g = \langle u, v \rangle \in E_n} (1 + \epsilon_g^2 \sigma_u \sigma_v).$$

By (4.4), this is the partition function of an Ising model on \mathbb{H}_n with (possibly complex) weights.

Let $e = \langle u, v \rangle$, $f = \langle x, y \rangle$ be distinct edges in E_n . Motivated by Section 4.3 and the discussion of the two-edge correlation $\langle \sigma_e \sigma_f \rangle_n$ of the 1-2 model, we define

$$(4.11) \quad \sigma(e, f) = \frac{1}{Z_n(I)} \sum_{\sigma^e \in \Sigma^e} \sum_{\sigma^v \in \Sigma^v} \sigma_e \sigma_f \prod_{v \in V_n} (1 + \epsilon_a \sigma_v \sigma_{v,a}) (1 + \epsilon_b \sigma_v \sigma_{v,b}) (1 + \epsilon_c \sigma_v \sigma_{v,c}).$$

By (4.9)–(4.10), this equals

$$(4.12) \quad \frac{1}{Z_n(I)} 2^{|E_n|} \sum_{\sigma^v \in \Sigma^v} \frac{\epsilon_e (\sigma_u + \sigma_v) \epsilon_f (\sigma_x + \sigma_y)}{(1 + \epsilon_e^2 \sigma_u \sigma_v) (1 + \epsilon_f^2 \sigma_x \sigma_y)} \prod_{g=\langle u,v \rangle \in E_n} (1 + \epsilon_g^2 \sigma_u \sigma_v) \\ = \sum_{\sigma^v \in \Sigma^v} D_{e,f}(\sigma^v) w(\sigma^v) / \sum_{\sigma^v \in \Sigma^v} w(\sigma^v),$$

where

$$w(\sigma^v) = \prod_{g=\langle u,v \rangle \in E_n} (1 + \epsilon_g^2 \sigma_u \sigma_v), \\ D_{e,f}(\sigma^v) = \frac{\epsilon_e (\sigma_u + \sigma_v) \epsilon_f (\sigma_x + \sigma_y)}{(1 + \epsilon_e^2 \sigma_u \sigma_v) (1 + \epsilon_f^2 \sigma_x \sigma_y)}, \quad e = \langle u, v \rangle, \quad f = \langle x, y \rangle.$$

We interpret $D_{e,f}(\sigma^v)$ as 0 when its denominator is 0. Since $\sigma_1 + \sigma_2 = 0$ when $\sigma_1 \sigma_2 = -1$, we may write

$$(4.13) \quad D_{e,f}(\sigma^v) = \frac{\epsilon_e (\sigma_u + \sigma_v) \epsilon_f (\sigma_x + \sigma_y)}{(1 + \epsilon_e^2) (1 + \epsilon_f^2)}.$$

If the weights $w(\sigma^v)$ are real and non-negative (which they are not in general), the ratio on the right side of (4.12) may be interpreted as an expectation. This observation will be used in Section 7.

By inspection of (4.10), if $\epsilon_g^2 = \pm 1$ for some $g \in \{a, b, c\}$, then zero mass is placed on configurations σ for which there exists an edge $\langle u, v \rangle$ of type g with $\sigma_u \sigma_v = \mp 1$. We turn to the special case of (4.6) and (4.2) with $ABC \neq 0$. Then

$$(4.14) \quad \epsilon_a^2 = \begin{cases} -1 & \text{if and only if } a^2 = b^2 + c^2, \\ 1 & \text{if and only if } bc = 0, \end{cases}$$

and similarly for ϵ_b , ϵ_c . Note in this case that $\sigma(e, f) = \langle \sigma_e \sigma_f \rangle_n$, the two-edge function for the associated 1-2 model.

5. DIMER REPRESENTATION OF THE 1-2 MODEL

5.1. The decorated dimer model. Let $\mathbb{H}_{n,\Delta} = (V_{n,\Delta}, E_{n,\Delta})$ be the decorated toroidal graph derived from \mathbb{H}_n and illustrated on the right of Figure 5.1. It was shown in [20] that there is a correspondence between 1-2 configurations on \mathbb{H}_n and

dimer configurations on $\mathbb{H}_{n,\Delta}$. This correspondence is summarized in the figure caption, and a more detailed description follows.

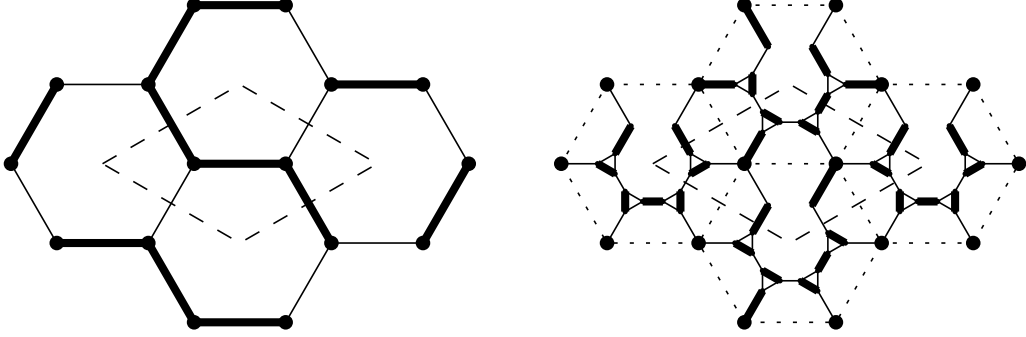


FIGURE 5.1. Part of a 1-2 configuration on \mathbb{H}_n , and the corresponding dimer (sub)configuration on $\mathbb{H}_{n,\Delta}$. When two edges with a common vertex of \mathbb{H}_n have the same state in the 1-2 model, the corresponding ‘bisector edge’ is present in the dimer configuration. The states of the bisector edges determine the dimer configuration on the rest of $\mathbb{H}_{n,\Delta}$. The edges of $\mathbb{H}_{n,\Delta}$ are allocated weights consistently with the 1-2 weights of Figure 2.2. The central lozenge is expanded in Figure 5.3.

Let σ be a 1-2 configuration on \mathbb{H}_n , and let $v \in V_n (\subseteq V_{n,\Delta})$. The vertex v has three incident edges in $\mathbb{H}_{n,\Delta}$, which are bisectors of the three angles of \mathbb{H}_n at v . Such a *bisector edge* is present in the dimer configuration on $\mathbb{H}_{n,\Delta}$ if and only if the two edges of the corresponding angle have the same σ -state, that is, either both or neither are present. The states of the bisector edges determine the dimer configuration on the entire $\mathbb{H}_{n,\Delta}$. Note that the 1-2 configurations σ and $-\sigma$ generate the same dimer configuration, denoted D_σ .

To the edges of $\mathbb{H}_{n,\Delta}$ we allocate weights as follows: edge $e = \langle i, j \rangle$ is allocated weight $w_{i,j}$ where

$$(5.1) \quad w_{i,j} = \begin{cases} a & \text{if } e \text{ is a horizontal bisector edge,} \\ b & \text{if } e \text{ is a NW/SE bisector edge,} \\ c & \text{if } e \text{ is a NE/SW bisector edge,} \\ 1 & \text{otherwise.} \end{cases}$$

The weight of a dimer configuration is the product of the weights of present edges.

To each 1-2 configuration σ on \mathbb{H}_n , there corresponds thus a unique dimer configuration on $\mathbb{H}_{n,\Delta}$. The converse is more complicated, and we preface the following

discussion with the introduction of the planar graph \mathbb{H}'_n , derived from \mathbb{H}_n by a process of ‘unwrapping’ the torus.

Let \mathbb{H}'_n be the planar graph obtained from \mathbb{H}_n by cutting through the two homology cycles γ_x and γ_y of the torus, as illustrated in Figure 5.2. That is, \mathbb{H}'_n may be viewed as the set of edges that intersect the region marked in Figure 5.2 (in which $n = 4$ and the central edge is labelled $\langle u, v \rangle$). We may consider \mathbb{H}'_n as a ‘partial-graph’ $\mathbb{H}'_n = (V_n, \tilde{E}_n, H_n)$, where V_n is the vertex set, \tilde{E}_n is the ‘internal’ edge set, and H_n is the set of half-edges having one endpoint in V_n and one outside V_n . We write H_x^1 and H_x^2 (respectively, H_y^1, H_y^2) for the sets of half-edges that cross the upper left and lower right sides (respectively, upper right and lower left sides) of the diamond of Figure 5.2. Let $H_u = H_u^1 \cup H_u^2$ for $u = x, y$.

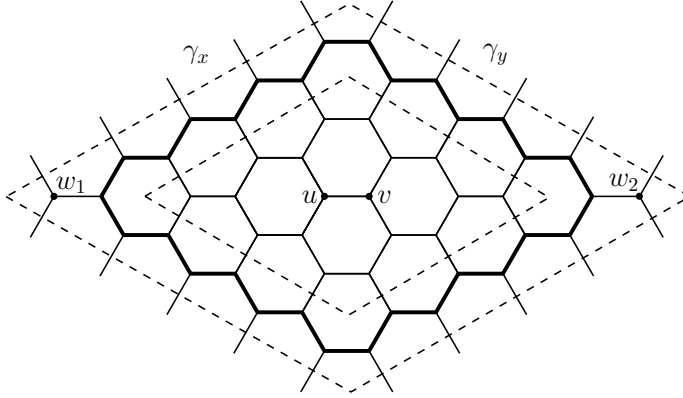


FIGURE 5.2. The $n \times n$ ‘diamond’ of \mathbb{H} , with $n = 4$. The region \mathbb{H}'_n comprises all edges and half-edges that intersect the larger diamond. The annulus between the given boundaries comprises a cycle C_n (drawn above in bold), and two further edges incident with the w_i .

A 1-2 configuration on \mathbb{H}'_n is a subset of edges and half-edges such that, for $v \in V_n$, the total number of edges and half-edges that are incident to v is either 1 or 2. It is explained in [20, p. 4] that dimer configurations on $\mathbb{H}_{n,\Delta}$ are in one-to-two correspondence to 1-2 configurations on \mathbb{H}'_n satisfying any of the following (pairwise exclusive) conditions:

- (ss) for $e \in H_x \cup H_y$, the two corresponding half-edges $e^1 \in H_x^1 \cup H_y^1, e^2 \in H_x^2 \cup H_y^2$ have the same state (either both are present or neither is present);
- (os) for $e \in H_x$, the two corresponding half-edges $e^1 \in H_x^1, e^2 \in H_x^2$ have the opposite states (exactly one of them is present); for $e \in H_y$, the two corresponding half-edges $e^1 \in H_y^1, e^2 \in H_y^2$ have the same state;

- (so) for $e \in H_x$, the two corresponding half-edges $e^1 \in H_x^1$, $e^2 \in H_x^2$ have the same state; for $e \in H_y$, the two corresponding half-edges $e^1 \in H_y^1$, $e^2 \in H_y^2$ have the opposite states;
- (oo) for $e \in H_x \cup H_y$, the two corresponding half-edges $e^1 \in H_x^1 \cup H_y^1$, $e^2 \in H_x^2 \cup H_y^2$ have the opposite states.

We refer to the above as the *mixed boundary condition* on \mathbb{H}'_n .

The above mixed boundary condition is more permissive than the periodic condition that gives rise to 1-2 configurations on the toroidal graph \mathbb{H}_n , although the difference turns out to be invisible in the infinite-volume limit (see Theorem 6.2).

5.2. The spectral curve of the dimer model. We turn now to the spectral curve of the above weighted dimer model on $\mathbb{H}_{n,\Delta}$. The reader is referred to [21] for relevant background, and to [20, Sect. 3] for further details of the following summary.

The fundamental domain of $\mathbb{H}_{n,\Delta}$ is the central lozenge of Figure 5.1, as expanded in Figure 5.3. The edges of $\mathbb{H}_{n,\Delta}$ are oriented as in the latter figure. It is easily checked that this orientation is ‘clockwise odd’, in the sense that any face of $\mathbb{H}_{n,\Delta}$, when traversed clockwise, contains an odd number of edges oriented in the corresponding direction. The fundamental domain has 16 vertices, and its weighted adjacency matrix (or ‘Kasteleyn matrix’) is the 16×16 matrix $\mathbf{B} = (b_{i,j})$ with

$$b_{i,j} = \begin{cases} w_{i,j} & \text{if } \langle i, j \rangle \text{ is oriented from } i \text{ to } j, \\ -w_{i,j} & \text{if } \langle i, j \rangle \text{ is oriented from } j \text{ to } i, \\ 0 & \text{if there is no edge between } i \text{ and } j, \end{cases}$$

where $w_{i,j}$ is given by (5.1). From \mathbf{B} we obtain a *modified adjacency* (or ‘Kasteleyn’) matrix $\mathbf{B}(z, w)$ as follows.

We may consider the graph of Figure 5.3 as being embedded in a torus, that is, we identify the upper left boundary and the lower right boundary, and also the upper right boundary and the lower left boundary, as illustrated in the figure by dashed lines.

Let $w, z \in \mathbb{C}$ be non-zero. We orient each of the four boundaries of Figure 5.3 (denoted by dashed lines) from their lower endpoint to their upper endpoint. The ‘left’ and ‘right’ of an oriented portion of a boundary are as viewed by a person traversing in the given direction.

Each edge $\langle u, v \rangle$ crossing a boundary corresponds to two entries in the weighted adjacency matrix, indexed (u, v) and (v, u) . If the edge starting from u and ending at v crosses an upper-left/lower-right boundary from left to right (respectively, from right to left), we modify the adjacency matrix by multiplying the entry (u, v) by z (respectively, z^{-1}). If the edge starting from u and ending at v crosses an upper-right/lower-left boundary from left to right (respectively, from right to left), in the modified adjacency matrix, we multiply the entry by w (respectively, w^{-1}). We

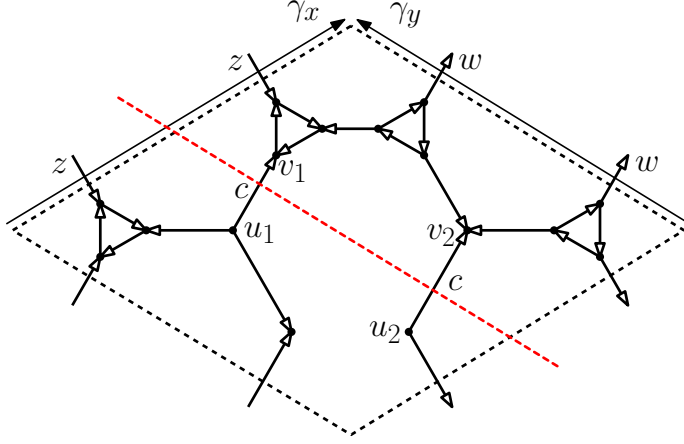


FIGURE 5.3. A single fundamental domain of the decorated graph $\mathbb{H}_{n,\Delta}$ obtained from the central lozenge of Figure 5.1. See that figure for an illustration of the relationship between this fundamental domain and the original hexagonal lattice \mathbb{H} . Note the homology cycles γ_x, γ_y of the torus, and also the two weight- c edges crossed by the central dashed line.

modify the entry (v, u) in the same way. The ensuing matrix is denoted $\mathbf{B}(z, w)$, for a definitive expression of which, the reader is referred to [20, Sect. 3].

The *characteristic polynomial* is given (using Mathematica or otherwise) by

$$(5.2) \quad P(z, w) = \det \mathbf{B}(z, w) = f(a, b, c; w, z),$$

where

$$\begin{aligned} f(a, b, c; w, z) = & a^4 + b^4 + c^4 + 6a^2b^2 + 6a^2c^2 + 6b^2c^2 - 2ab \left(z + \frac{1}{z} \right) (a^2 + b^2 - c^2) \\ & - 2ac \left(w + \frac{1}{w} \right) (a^2 + c^2 - b^2) - 2bc \left(\frac{z}{w} + \frac{w}{z} \right) (b^2 + c^2 - a^2). \end{aligned}$$

The *spectral curve* is the zero locus of the characteristic polynomial, that is, the set of roots of $P(z, w) = 0$. It is proved in [20, Lemma 3.2] that the intersection of $P(z, w) = 0$ with the unit torus \mathbb{T}^2 is either empty or a single real point $(1, 1)$. Moreover, in the situation when $P(1, 1) = 0$, the zero $(1, 1)$ has multiplicity 2. It will be important later to identify the conditions under which $P(1, 1) = 0$.

Proposition 5.1. *Let $a, b > 0$ and $c \geq 0$.*

(a) *If any of the following hold,*

$$(i) \quad \sqrt{a} = \sqrt{b} + \sqrt{c}, \quad (ii) \quad \sqrt{b} = \sqrt{c} + \sqrt{a}, \quad (iii) \quad \sqrt{c} = \sqrt{a} + \sqrt{b},$$

the curve $P(z, w) = 0$ intersects the unit torus $\mathbb{T}^2 = \{(z, w) : |z| = 1, |w| = 1\}$ at the unique point $(1, 1)$.

(b) If none of (i)–(iii) hold, the curve does not intersect the unit torus.

Proof. The intersection of $P(z, w) = 0$ with \mathbb{T}^2 can only be either empty or a single point $(1, 1)$, by [20, Lemma 3.2]. Moreover, since

$$(5.3) \quad f(a, b, c; 1, 1) = (a^2 + b^2 + c^2 - 2ab - 2bc - 2ac)^2,$$

we have that $f(a, b, c; 1, 1) = 0$ if and only if $\sqrt{a} \pm \sqrt{b} \pm \sqrt{c} = 0$. \square

We note for future use that

$$(5.4) \quad P(1, 1) = f(a, b, c; 1, 1) = \frac{1}{4}[(A^2 + B^2 + C^2 - 1)(a + b + c)^2]^2,$$

where A, B, C are as in (4.2).

6. INFINITE-VOLUME LIMITS

This paper is directed primarily at the asymptotic behaviour of the two-edge correlation function of the 1-2 model, rather than at the existence and multiplicity of infinite-volume measures. Partial results in the latter direction are reported in this section. In Section 6.1, the weak limit of the toroidal 1-2 measure is proved via a relationship with the dimer model on a decorated graph. In Section 6.2 we prove the non-uniqueness of Gibbs measures for the ‘low temperature’ 1-2 model. The existence of the infinite-volume free energy is proved in Section 6.3.

6.1. Toroidal limit measure. The 1-2 model may be studied via the dimer representation of Section 5. The dimer convergence theorem of [20] is as follows.

Theorem 6.1. [20, Prop. 3.3] *Consider the dimer measure $\delta_{n,\Delta}$ on $\mathbb{H}_{n,\Delta}$ with parameters $a, b, c > 0$. The limit measure $\delta_\Delta := \lim_{n \rightarrow \infty} \delta_{n,\Delta}$ exists and is translation-invariant and ergodic.*

Let μ_n^{mix} (respectively, μ_n) be the 1-2 probability measure on \mathbb{H}'_n (respectively, on the toroidal \mathbb{H}_n) with parameters a, b, c and mixed boundary condition. By the results of [20] and the invariance of μ_n^{mix} under sign changes,

$$(6.1) \quad \mu_n^{\text{mix}}(\sigma) = \mu_n^{\text{mix}}(-\sigma) = \frac{1}{2}\delta_{n,\Delta}(D_\sigma),$$

where D_σ is the dimer configuration on $\mathbb{H}_{n,\Delta}$ corresponding to the 1-2 configuration σ on \mathbb{H}'_n . Since the topology of weak convergence may be given in terms of finite-dimensional cylinder events, the weak convergence $\delta_{n,\Delta} \Rightarrow \delta_\Delta$ entails the weak convergence of μ_n^{mix} to some probability measure μ^{mix} on \mathbb{H} . By Theorem 6.1, μ^{mix} is translation-invariant. It is noted at [20, p. 17] that the ergodicity of δ_Δ does not imply that of μ^{mix} .

Theorem 6.2. *Let $a, b, c > 0$. The limit $\mu_\infty := \lim_{n \rightarrow \infty} \mu_n$ exists and satisfies $\mu_\infty = \mu^{\text{mix}}$. In particular, for edges e, f of \mathbb{H} , the limit*

$$(6.2) \quad \langle \sigma_e \sigma_f \rangle := \lim_{n \rightarrow \infty} \langle \sigma_e \sigma_f \rangle_n$$

exists.

Proof. Let $\Omega_{n,\Delta}$ be the sample space of the dimer model on $\mathbb{H}_{n,\Delta}$. Let δ_n^{ev} be the probability measure of the dimer model on $\mathbb{H}_{n,\Delta}$ on the subspace $\Omega_{n,\Delta}^{\text{ev}}$ of configurations with the property that, along each of the two zigzag paths of \mathbb{H} that are neighbouring and parallel to γ_x and γ_y , there are an even number of present bisector edges.

As explained above (see also [20]), elements of $\Omega_{n,\Delta}$ correspond to 1-2 model configurations on \mathbb{H}'_n with the mixed boundary condition, and of $\Omega_{n,\Delta}^{\text{ev}}$ to 1-2 model configurations on the toroidal graph \mathbb{H}_n . We show next that

$$(6.3) \quad \delta_{n,\Delta}^{\text{ev}} \Rightarrow \delta_\Delta,$$

where $\delta_\Delta := \lim_{n \rightarrow \infty} \delta_{n,\Delta}$ is given in Theorem 6.1.

Let $Z_{n,\Delta}$ (respectively, $Z_{n,\Delta}^{\text{ev}}$) be the partition function of $\Omega_{n,\Delta}$ (respectively, $\Omega_{n,\Delta}^{\text{ev}}$), and let $K_n(z, w)$ be the modified Kasteleyn matrix of $\mathbb{H}_{n,\Delta}$ (see [20] and Section 5.2). As explained in [24, Sect. 4B], for $z, w \in \{-1, 1\}$, $\text{Pf } K_n(z, w)$ is a linear combination of partition functions of dimer configurations of four different classes, depending on the parity of the present edges along the two zigzag paths winding around the torus. In particular, by [24, Table 1, Sect. 4B], when n is even,

$$Z_{n,\Delta}^{\text{ev}} = \frac{1}{4} \left[\text{Pf } K_n(1, 1) + \text{Pf } K_n(-1, 1) + \text{Pf } K_n(1, -1) + \text{Pf } K_n(-1, -1) \right].$$

Let $e_i = \langle u_i, v_i \rangle$, $1 \leq i \leq k$, be edges of $\mathbb{H}_{n,\Delta}$, and let $M(e_1, \dots, e_k)$ be the event that every e_i is occupied by a dimer. Let $w_i > 0$ be the edge weight of e_i . Then

$$\begin{aligned} & \delta_n^{\text{ev}}(M(e_1, \dots, e_k)) \\ &= \prod_{i=1}^k w_{e_i} \left| \frac{\text{Pf } \widehat{K}_n(1, 1) + \text{Pf } \widehat{K}_n(-1, 1) + \text{Pf } \widehat{K}_n(1, -1) + \text{Pf } \widehat{K}_n(-1, -1)}{\text{Pf } K_n(1, 1) + \text{Pf } K_n(-1, 1) + \text{Pf } K_n(1, -1) + \text{Pf } K_n(-1, -1)} \right|, \end{aligned}$$

where \widehat{K}_n is the submatrix of K_n obtained by removing rows and columns indexed by $u_1, v_1, \dots, u_k, v_k$. As in [4, Thm 4],

(6.4)

$$\begin{aligned} & \delta_{n,\Delta}(M(e_1, \dots, e_k)) \\ &= \prod_{i=1}^k w_{e_i} \left| \frac{-\text{Pf } \widehat{K}_n(1, 1) + \text{Pf } \widehat{K}_n(-1, 1) + \text{Pf } \widehat{K}_n(1, -1) + \text{Pf } \widehat{K}_n(-1, -1)}{-\text{Pf } K_n(1, 1) + \text{Pf } K_n(-1, 1) + \text{Pf } K_n(1, -1) + \text{Pf } K_n(-1, -1)} \right|. \end{aligned}$$

As in the proof of [4, Thm 6], $\delta_{n,\Delta}^{\text{ev}}(M(e_1, \dots, e_k))$ and $\delta_{n,\Delta}(M(e_1, \dots, e_k))$ converge as $n \rightarrow \infty$ to the same complex integral. Since the events $M(e_1, \dots, e_k)$ generate the product σ -field, we deduce (6.3).

Finally, we deduce the claim of the theorem. An *even* (respectively, *odd*) *correlation function* is an expectation of the form $\langle \sigma_A \rangle$, with $\sigma_A = \prod_{e \in A} \sigma_e$ where A is a finite set of edges of \mathbb{H} with even (respectively, odd) cardinality. In order that $\mu_n \Rightarrow \mu^{\text{mix}}$, it suffices that the correlation functions of μ_n and μ_n^{mix} have the same limit. By invariance under sign change, the odd correlation functions equal 0.

The relationship between a 1-2 measure μ and the corresponding dimer measure δ is as follows. Let e_1, \dots, e_k be bisector edges of $\mathbb{H}_{n,\Delta}$, and let $S(e_1, \dots, e_k)$ be the event that every e_i separates two edges of \mathbb{H}_n with the same 1-2 state. Using the correspondence between 1-2 and dimer configurations,

$$\mu(S(e_1, \dots, e_k)) = \delta(M(e_1, \dots, e_k)).$$

Let $k \geq 1$, let e_1, e_2, \dots, e_{2k} be distinct edges of \mathbb{H}_n , and write $\sigma_i = \sigma_{e_i}$. Then

$$(6.5) \quad \langle \sigma_1 \cdots \sigma_{2k} \rangle_\mu = 1 - 2\mu(\sigma_1 \cdots \sigma_{2k} = -1).$$

For $i = 2, 3, \dots, 2k$, let π_i be a self-avoiding path between the midpoints of e_1 and e_i comprising edges of \mathbb{H}_n and two half-edges, and let \mathcal{A}_i be the event that the number of *absent* bisector edges encountered along π_i is odd. As we move along π_i in the 1-2 model, the edge-state changes at a given vertex if and only if the corresponding bisector edge is absent. Therefore, $\sigma_1 \sigma_i = -1$ if and only if \mathcal{A}_i occurs, so that

$$(6.6) \quad \langle \sigma_e \sigma_f \rangle_\mu = \mu(\overline{\mathcal{A}_i}) - \mu(\mathcal{A}_i).$$

Let \mathcal{A} be the event that the set $I = \{i : \mathcal{A}_i \text{ occurs}\}$ has odd cardinality. Since $I = \{i : \sigma_1 \neq \sigma_i\}$, we have that

$$(6.7) \quad \mu(\sigma_1 \cdots \sigma_{2k} = -1) = \delta(\mathcal{A}).$$

We return to the measures μ_n and μ_n^{mix} . By (6.3)–(6.7), the even correlation functions of μ_n and μ_n^{mix} are convergent as $n \rightarrow \infty$, with equal limits. It follows that $\mu_n \Rightarrow \mu_\infty$ where $\mu_\infty = \mu^{\text{mix}}$. \square

6.2. Non-uniqueness of Gibbs measures. We show the existence of at least two Gibbs measures (that is, ‘phase coexistence’) for the ‘low temperature’ 1-2 model on \mathbb{H} . Let Σ be the set of 1-2 configurations on the infinite lattice \mathbb{H} , and let $\mathcal{G} = \mathcal{G}(a, b, c)$ be the set of probability measures on Σ that satisfy the appropriate DLR condition. (We omit the details of DLR measures here, instead referring the reader to the related discussions of [3, Sect. 2.3] and [12, Sect. 4.4].) Since Σ is compact, by Prohorov’s theorem [2, Sect. 1.5], every sequence of probability measures on Σ has a convergent subsequence. It may be shown that any weak limit of finite-volume 1-2 measures lies in \mathcal{G} , and hence $\mathcal{G} \neq \emptyset$.

Theorem 6.3. *Let $a \geq b > 0$. For almost every c satisfying either $0 < \sqrt{c} < \sqrt{a} - \sqrt{b}$ or $\sqrt{c} > \sqrt{a} + \sqrt{b}$, we have that $|\mathcal{G}| \geq 2$.*

Proof. This proof is inspired by that of [3, Thm 6.2], and it makes use of Theorem 3.1, the proof of which has been deferred to Section 8. Let e be a given horizontal edge of \mathbb{H}_n , and let f_m be an edge satisfying (3.1) such that $\pi(e, f_m)$ has length m . By Theorem 3.1(b) and translation invariance, for almost every c satisfying the given inequalities, there exists $\alpha > 0$ such that

$$(6.8) \quad \lim_{m \rightarrow \infty} \langle \sigma_e \sigma_{f_m} \rangle^2 = \alpha^2,$$

where $\langle \sigma_e \sigma_f \rangle$ is the limiting two-edge correlation as $n \rightarrow \infty$ (see Theorem 6.2). It suffices to show that, subject to (6.8), $|\mathcal{G}| \geq 2$.

By Theorem 6.2, $\langle \sigma_e \sigma_f \rangle$ converges to either α or to $-\alpha$. Assume the first, that is

$$\lim_{m \rightarrow \infty} \langle \sigma_e \sigma_{f_m} \rangle = \alpha;$$

the proof is essentially the same in the second case.

By the invariance of μ_∞ under sign change of the configuration,

$$\begin{aligned} \lim_{m \rightarrow \infty} \mu_\infty(\sigma_e = 1 \mid \sigma_{f_m} = 1) &= \frac{1}{2}(1 + \alpha), \\ \lim_{m \rightarrow \infty} \mu_\infty(\sigma_e = 1 \mid \sigma_{f_m} = -1) &= \frac{1}{2}(1 - \alpha). \end{aligned}$$

Find M such that

$$\begin{aligned} \mu_\infty(\sigma_e = 1 \mid \sigma_{f_m} = -1) &< \frac{1}{2}(1 - \frac{1}{2}\alpha) \\ &< \frac{1}{2}(1 + \frac{1}{2}\alpha) < \mu_\infty(\sigma_e = 1 \mid \sigma_{f_m} = 1), \quad m \geq M. \end{aligned}$$

We may find an increasing subsequence $(r_m : m \geq M)$ such that

$$\begin{aligned} \mu_{r_m}(\sigma_e = 1 \mid \sigma_{f_m} = -1) &< \frac{1}{2}(1 - \frac{1}{3}\alpha) \\ &< \frac{1}{2}(1 + \frac{1}{3}\alpha) < \mu_{r_m}(\sigma_e = 1 \mid \sigma_{f_m} = 1), \quad m \geq M. \end{aligned}$$

Let μ^+ (respectively, μ^-) be a subsequential limit of $\mu_{r_m}(\cdot \mid \sigma_{f_m} = 1)$ (respectively, $\mu_{r_m}(\cdot \mid \sigma_{f_m} = -1)$), so that

$$\mu^+(\sigma_e = 1) > \mu^-(\sigma_e = 1).$$

In particular, $\mu^+ \neq \mu^-$. Since $|e - f_m| \rightarrow \infty$ as $m \rightarrow \infty$, the measures μ^\pm satisfy the DLR condition, and therefore they lie in \mathcal{G} . \square

6.3. Free energy. A *boundary condition* \mathcal{B}_n is a configuration on the half-edges H_n of the planar graph $\mathbb{H}'_n = (V_n, \tilde{E}_n, H_n)$, in the notation of Section 6.1. Let $Z_n(a, b, c, \mathcal{B}_n)$ be the partition function of the 1-2 model on \mathbb{H}'_n with parameters a, b, c and boundary condition \mathcal{B}_n (as in (4.1), say). The free energy, for given a, b, c and boundary conditions ($\mathcal{B}_n : n \geq 1$), is defined to be

$$(6.9) \quad \mathcal{F}(a, b, c, (\mathcal{B}_n)) := \lim_{n \rightarrow \infty} \frac{1}{|V_n|} \log Z_n(a, b, c, \mathcal{B}_n),$$

whenever the limit exists.

Proposition 6.4. *Let $(a, b, c) \neq (0, 0, 0)$. The free energy of (6.9) exists and is independent of the choice of boundary conditions (\mathcal{B}_n) . Moreover, up to a smooth additive constant, it satisfies*

$$(6.10) \quad \mathcal{F}(a, b, c) = \frac{1}{4\pi^2} \iint_{[0, 2\pi]^2} \log P(e^{i\theta}, e^{i\phi}) d\theta d\phi,$$

where P is given in (5.2).

Proof. The correspondence between 1-2 model configurations on \mathbb{H}'_n (with the mixed boundary condition) and dimer configurations on $\mathbb{H}_{n, \Delta}$ was explained in Section 6.1. It follows that the free energy of that 1-2 model is the same as that of the corresponding dimer model. The expression (6.10) follows for that case from a general argument used to compute the free energy of this dimer model, given that either the spectral curve does not intersect the unit torus, or the intersection is a unique real point of multiplicity 2. See Proposition 5.1 and also [17, Thm 3.5] and [4, Thm 1].

Next we prove that the free energy of (6.9) is independent of the choice of (\mathcal{B}_n) . To this end, we consider the boxes \mathbb{H}'_n and \mathbb{H}'_{n-2} illustrated in Figure 5.2. We claim that, for any boundary condition on \mathbb{H}'_n (that is, any present/absent configuration on H_n) and any 1-2 model configuration on \mathbb{H}'_{n-2} (so that the edge-states on $\tilde{E}_{n-2} \cup H_{n-2}$ are given), there exists a configuration on $\tilde{E}_n \setminus (\tilde{E}_{n-2} \cup H_{n-2})$ such that the composite configuration is a 1-2 configuration on \mathbb{H}'_n .

This claim is shown as follows. Consider a given boundary condition on H_n and a 1-2 configuration on \mathbb{H}'_{n-2} . The vertex-set $V_n \setminus V_{n-2}$ forms a cycle C_n with even length, together with two further vertices w_1, w_2 at the left and right corners, see Figure 5.2. From C_n we select a perfect matching. By considering the various possibilities, we may see that it is always possible to allocate states to the two edges between C_n and the w_i in such a way that, in the resulting composite configuration, each w_i has degree either 1 or 2.

Let \mathcal{B}_n^0 be the *free boundary condition*, under which no half-edge is present. We have that

$$|\log Z_n(a, b, c, \mathcal{B}_n) - \log Z_{n-2}(a, b, c, \mathcal{B}_{n-2}^0)| \leq |V_n \setminus V_{n-2}|K,$$

for some $K = K(a, b, c) > 0$ and all \mathcal{B}_n . Divide by $|V_n|$ and let $n \rightarrow \infty$ to obtain the claim. The theorem follows on noting that the number of boundary configurations is $2^{|H_n|}$, and $|H_n|/|V_n| \rightarrow 0$ as $n \rightarrow \infty$. \square

7. EXPONENTIAL DECAY UNDER THE ACUTE TRIANGLE CONDITION

Three reals a, b, c are said to satisfy the *acute triangle condition* if the following inequalities hold simultaneously:

$$(7.1) \quad a, b, c > 0, \quad a^2 < b^2 + c^2, \quad b^2 < c^2 + a^2, \quad c^2 < a^2 + b^2.$$

The main result of this section is Theorem 3.2, which we expand as follows.

Theorem 7.1. *Consider the 1-2 model on \mathbb{H}_n with parameters satisfying the acute triangle condition (7.1). The limit $\langle \sigma_e \sigma_f \rangle$ of (6.2) decays exponentially fast to 0 as $|e - f| \rightarrow \infty$.*

The remainder of this section is devoted to the proof of this theorem. The existence of the limit $\langle \sigma_e \sigma_f \rangle$ follows by Theorem 6.2. Without loss of generality, we may assume that $a \geq b \geq c > 0$, in which case (7.1) is equivalent to

$$(7.2) \quad a^2 < b^2 + c^2.$$

Let A, B, C be given by (4.2), and note that $A, B, C < 0$. The partition function of the 1-2 model on $\mathbb{H}_n = (V_n, E_n)$ can be viewed as the marginal of the enhanced Ising model of (4.5) with the ϵ_g given by (4.6). Note that the ϵ_g are purely imaginary, so that the Ising model of (4.10) is antiferromagnetic.

It is standard that an antiferromagnetic Ising model on a bipartite graph may be transformed into a ferromagnetic system by flipping the signs of a family of spins, see [11, p. 17]. The graph \mathbb{H}_n is bipartite with vertex-classes coloured black and white (see the discussion around Figure 2.2). We will retain the spins of white vertices, while switching the signs of spins of black vertices. Thus, exactly one endpoint of each edge has a switched spin-value. We retain the notation σ^v , and ask the reader to remember that black vertex-spins have been flipped.

By (4.10), in the flipped system,

$$(7.3) \quad Z_n(I) = 2^{|E_n|} \sum_{\sigma^v \in \Sigma^v} \prod_{g=\langle u,v \rangle \in E_n} (1 + t_g \sigma_u \sigma_v),$$

where $t_g > 0$ is given by

$$t_g = -\epsilon_g^2 = \begin{cases} -BC/A & \text{if } g \text{ is horizontal,} \\ -AC/B & \text{if } g \text{ is NW/SE,} \\ -AB/C & \text{if } g \text{ is NE/SW.} \end{cases}$$

Under (7.1), we have $0 < t_e < 1$ for $e \in E_n$. Let

$$(7.4) \quad \tanh J_e = t_e,$$

so that $J_e \in (0, \infty)$. By (4.4), the partition function $Z_n(I)$ is the same (up to a multiplicative factor) as that of a ferromagnetic Ising model on \mathbb{H}_n with coupling constant J_e on the edge $e \in E_n$.

Let $e = \langle u, v \rangle$, $f = \langle x, y \rangle$ be distinct edges in E_n such that u, x are white and v, y are black. By (4.11)–(4.13),

$$(7.5) \quad \langle \sigma_e \sigma_f \rangle_n = -\langle D'_{e,f}(\sigma^v) \rangle_n^I,$$

where $\langle \cdot \rangle_n^I$ denotes expectation with respect to the ferromagnetic Ising model of (7.3), and

$$(7.6) \quad D'_{e,f}(\sigma^v) = \frac{\sqrt{t_e t_f}(\sigma_u - \sigma_v)(\sigma_x - \sigma_y)}{(1 - t_e)(1 - t_f)}.$$

We show next that the above ferromagnetic Ising model is in its high-temperature phase. It will follow that $\langle \sigma_e \sigma_f \rangle \rightarrow 0$ exponentially fast in the limit as $|e - f| \rightarrow \infty$. Consider then a ferromagnetic Ising model with coupling constants βJ_e , where $\beta > 0$ denotes inverse temperature.

Lemma 7.2. *The critical inverse temperature β_c of the above ferromagnetic Ising model satisfies $\beta_c > 1$.*

Proof. It is standard that $0 < \beta_c < \infty$. The critical model on the hexagonal lattice \mathbb{H} corresponds to an isoradial embedding of \mathbb{H} in the plane, derived from a rhombic tiling, in which the local geometry is a function of the critical parameters (see, for example, [?, 7, 23]). This correspondence can be expressed as follows. The half-angle θ_e of the rhombus of an edge e satisfies

$$(7.7) \quad \tan(\tfrac{1}{2}\theta_e) = \tanh(\beta_c J_e).$$

The set of rhombi thus constructed forms a rhombic tiling of \mathbb{R}^2 if, for edges e_1, e_2, e_3 of \mathbb{H} with a common vertex,

$$\theta_{e_1}, \theta_{e_2}, \theta_{e_3} \in (0, \tfrac{1}{2}\pi), \quad \theta_{e_1} + \theta_{e_2} + \theta_{e_3} = \pi.$$

We compute the θ_{e_i} according to (7.4) and (7.7) with β_c replaced by 1, to find that $\tfrac{1}{2}\theta_{e_i} \in (0, \tfrac{1}{4}\pi)$ and

$$(7.8) \quad \tan(\tfrac{1}{2}\theta_{e_1}) = -\frac{BC}{A}, \quad \tan(\tfrac{1}{2}\theta_{e_2}) = -\frac{AC}{B}, \quad \tan(\tfrac{1}{2}\theta_{e_3}) = -\frac{AB}{C}.$$

In order that $\beta_c > 1$, it suffices that

$$(7.9) \quad \tfrac{1}{2}\theta_{e_1} + \tfrac{1}{2}\theta_{e_2} + \tfrac{1}{2}\theta_{e_3} < \tfrac{1}{2}\pi \quad \text{subject to (7.1) and (7.8).}$$

By elementary trigonometry, the inequality of (7.9) holds if

$$-\frac{BC}{A} - \frac{AC}{B} - \frac{AB}{C} + ABC = \frac{-(AB)^2(1-C^2) - (BC)^2 - (AC)^2}{ABC} > 0,$$

$$1 - A^2 - B^2 - C^2 > 0.$$

The first inequality holds since $A, B, C < 0$ and $|C| < 1$, and the second may be checked by calculus using (7.2) and (4.2). \square

Proposition 7.3. *Subject to (7.2), the limit $\langle \sigma_e \sigma_f \rangle$ of (6.2) decays exponentially fast to zero as $|e - f| \rightarrow \infty$.*

Proof. A high-temperature Ising model in two dimensions has a unique Gibbs measure which has exponentially-decaying two-point function (see [1] or otherwise). \square

Proof of Theorem 7.1. This is an immediate consequence of Proposition 7.3. \square

8. PROOF OF THEOREM 3.1

The basic structure of the proof is as follows. As in Section 5, the 1-2 model may be represented as a dimer model on a certain decorated graph $\mathbb{H}_{n,\Delta}$ derived from \mathbb{H}_n . Subject to condition (3.1), the two-edge correlation $\langle \sigma_e \sigma_f \rangle_n$ of the 1-2 model may be represented in terms of certain cylinder probabilities of the dimer model. Using the theory of dimers, these probabilities may be expressed in terms of ratios of Pfaffians of block Toeplitz matrices, and a similar representation follows for the infinite-volume two-edge correlation $\langle \sigma_e \sigma_f \rangle$. By Widom's theorem [28, 29], the limit $\Lambda(a, b, c) := \lim_{|e-f| \rightarrow \infty} \langle \sigma_e \sigma_f \rangle^2$ exists, and furthermore Λ is analytic except when the spectral curve intersects the unit torus. This identifies the phases of the 1-2 model, and they may be identified as sub/supercritical via the extreme values of (3.2).

We assume henceforth that the edges e, f of \mathbb{H} satisfy the following condition:

$$(8.1) \quad \begin{aligned} &e \text{ and } f \text{ are midpoints of two NW/SE edges such that} \\ &\text{there exists a path } \pi = \pi(e, f) \text{ in } A\mathbb{H}_n \text{ from } e \text{ to } f \\ &\text{using only horizontal and NW/SE half-edges.} \end{aligned}$$

See Figure 8.1. The principal step in the proof is the following.

Theorem 8.1. *Let e, f be two edges satisfying (8.1), and let $a \geq b \geq 0$. The limit $\Lambda(a, b, c) := \lim_{|e-f| \rightarrow \infty} \langle \sigma_e \sigma_f \rangle^2$ is complex analytic in $c \geq 0$ except when $\sqrt{c} = \sqrt{a} - \sqrt{b}$ and $\sqrt{c} = \sqrt{a} + \sqrt{b}$.*

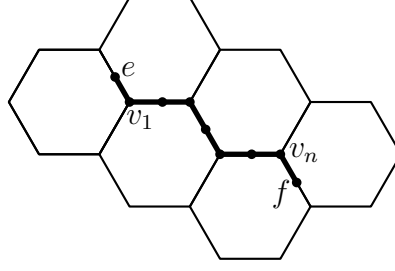


FIGURE 8.1. A path π comprising horizontal and NW/SE mid-edges, connecting the midpoints of two NW/SE edges e and f .

Proof of Theorem 3.1. Part (a) holds by Theorem 6.2. Let $a \geq b > 0$. By Theorem 8.1, the function $\Lambda_3(\cdot) := \Lambda(a, b, \cdot)$ is complex analytic on each of the intervals

$$\begin{aligned} C_1 &= [0, (\sqrt{a} - \sqrt{b})^2), \\ C_2 &= ((\sqrt{a} - \sqrt{b})^2, (\sqrt{a} + \sqrt{b})^2), \\ C_3 &= ((\sqrt{a} + \sqrt{b})^2, \infty). \end{aligned}$$

(That is to say, for $c \in C_i$ considered as a line in the complex plane, Λ_3 is analytic on some open neighbourhood of c .) By Theorem 7.1, $\Lambda_3(c) = 0$ when $c \in S := (\sqrt{a^2 - b^2}, \sqrt{a^2 + b^2})$. Since $S \subseteq C_2$ and Λ_3 is analytic on C_2 , the claim of part (c) follows. (The claim is trivial if $a = b$.)

We turn to part (b). Consider first the interval C_1 , and assume $a > b$. Since non-trivial analytic functions have only isolated zeros, it follows that: either $\Lambda_3 \equiv 0$ on C_1 , or Λ_3 is non-zero except possibly on a set of isolated points of C_1 . By (3.2), $\Lambda_3(0) = 1$, whence the latter holds.

By (3.2), $\langle \sigma_e \sigma_f \rangle = 1$ when $a = b = 0$ and $c = 1$. Since Λ_3 is analytic (and hence continuous) on C_3 , there exists $\alpha > 0$ such that $\Lambda(a, b, c) \geq \alpha$ in a small (real) neighbourhood of $(0, 0, 1)$. Since Λ depends only on the ratios $a : b : c$ (cf. (2.5)), we deduce that, for fixed $a, b > 0$ and sufficiently large c , we have $\Lambda_3(c) \geq \alpha > 0$. By Theorem 8.1, Λ_3 is analytic on C_3 , and the claim holds as above. \square

The remainder of the section is devoted to the proof of Theorem 8.1. We shall develop the notation and arguments of Section 6.1. Let μ_n^{mix} be the 1-2 measure on \mathbb{H}'_n with the mixed boundary condition of Section 6.1, and let $\mu^{\text{mix}} := \lim_{n \rightarrow \infty} \mu_n^{\text{mix}}$, as after Theorem 6.1. By Theorem 6.2, the 1-2 measure μ_n on \mathbb{H}_n satisfies $\mu_n \Rightarrow \mu_\infty = \mu^{\text{mix}}$ as $n \rightarrow \infty$.

Let e, f be edges of the hexagonal lattice \mathbb{H} satisfying (8.1). Let the path π of (8.1) traverse a total of $2k - 1$ edges and two half-edges, so that π passes $2k$ bisector

edges of the infinite decorated graph \mathbb{H}_Δ . We denote this set of bisector edges by

$$(8.2) \quad B = \{b_i = \langle u_i, v_i \rangle : i = 1, 2, \dots, k\},$$

where $v_i \in \pi$.

Our target is to represent $\langle \sigma_e \sigma_f \rangle$ as the Pfaffian of a truncated block Toeplitz matrix, as inspired by [15, Sect. 4.7]. A principal difference between [15] and the current work is that, whereas bipartite graphs are considered there and the determinants of weighted adjacency matrices are computed, in the current setting the graph is non-bipartite and we will compute Pfaffians.

To \mathbb{H}_Δ we assign a clockwise odd orientation as in Figure 5.3: the figure shows a clockwise odd orientation of $\mathbb{H}_{1,\Delta}$, embedded in a 1×1 torus, that lifts to a clockwise odd orientation of \mathbb{H}_Δ . As in (5.1), a horizontal (respectively, NW/SE, NE/SW) bisector edge of \mathbb{H}_Δ is assigned weight a (respectively, b, c), and all the other edges are assigned weight 1. The bisector edges $g_i = \langle u_i, v_i \rangle$ are oriented in such a way that each g_i is oriented from u_i to v_i in this clockwise-odd orientation.

Let K_n be the Kasteleyn matrix of $\mathbb{H}_{n,\Delta}$ (as in Section 5.2 and [20]), and let $|v|$ denote the index of the row and column of K_n corresponding to the vertex v . Assume that $|v_i| = |u_i| + 1$ for $1 \leq i \leq 2k$, and furthermore that

$$(8.3) \quad |u_1| < |v_1| < |u_2| < |v_2| < \dots < |u_k| < |v_k|.$$

Let K^{-1} be the infinite matrix whose entries are the limits of the entries of K_n^{-1} as $n \rightarrow \infty$. The existence of K^{-1} may be proved by an explicit diagonalization of K_n using periodicity, as in [8, Sect. 7] and [19].

We now construct the modified Kasteleyn matrix $K_1(z, w)$ of $\mathbb{H}_{1,\Delta}$ by multiplying the corresponding entries in its Kasteleyn matrix by z or z^{-1} (respectively, w or w^{-1}), according to the manner in which the edge crosses one of the two homology cycles γ_x, γ_y indicated in Figure 5.3. As remarked in Section 5.2, the characteristic polynomial $P(z, w) = \det K_1(z, w)$ is the function $f(a, b, c; w, z)$ of (5.2), see also [20, Lemma 9]. The intersection of the spectral curve $P(z, w) = 0$ and the unit torus \mathbb{T}^2 is given by Proposition 5.1.

Consider the toroidal graph $\mathbb{H}_{n,\Delta}$. Let γ_x, γ_y be homology cycles of the torus, which for definiteness we take to be shortest cycles composed of unions of boundary segments of fundamental domains as in Figure 5.3. Let $K_n(z, w)$ be the modified Kasteleyn matrix of $\mathbb{H}_{n,\Delta}$.

For $I \subseteq \{1, 2, \dots, 2k\}$, let M_I be the event that every b_i with $i \in I$ is present in the dimer configuration. Assume n is sufficiently large that

$$(8.4) \quad \text{for } 1 \leq i \leq 2k, \quad \text{the edge } b_i \text{ intersects neither } \gamma_x \text{ nor } \gamma_y.$$

For n even, as in (6.4),

(8.5)

$$\begin{aligned} \mu_\infty(M_I) &= \lim_{n \rightarrow \infty} \mu_n(M_I) \\ &= \lim_{n \rightarrow \infty} J_I \frac{-\text{Pf } \widehat{K}_{n,I}(1, 1) + \text{Pf } \widehat{K}_{n,I}(1, -1) + \text{Pf } \widehat{K}_{n,I}(-1, 1) + \text{Pf } \widehat{K}_{n,I}(-1, -1)}{-\text{Pf } K_n(1, 1) + \text{Pf } K_n(1, -1) + \text{Pf } K_n(-1, 1) + \text{Pf } K_n(-1, -1)}, \end{aligned}$$

where

$$(8.6) \quad J_I = \prod_{i \in I} [K_n]_{u_i, v_i},$$

and \widehat{A}_I denotes the submatrix of the matrix A after deletion of rows and columns corresponding to $\{u_i, v_i : i \in I\}$ (see [20, Thm 0.1]). Note that $\mu_\infty(M_\emptyset) = 1$.

The limit of (8.5) can be viewed as follows. Each monomial in the expansion of $\text{Pf } K_n(z, w)$, $z, w \in \{-1, 1\}$, corresponds to the product of edge-weights of a dimer configuration, but may have negative sign; the linear combination of $\text{Pf } K_n(1, 1)$, $\text{Pf } K_n(1, -1)$, $\text{Pf } K_n(-1, 1)$, and $\text{Pf } K_n(-1, -1)$ is chosen in such a way that the products of edge-weights of different dimer configurations correspond to monomials of the same sign. The numerator of (8.5) is the sum over dimer configurations containing every b_i , $i \in I$; this can be computed by the corresponding sum of monomials in the expansion of the denominator. Under (8.4), $[K_n]_{u_i, v_i} := [K_n(z, w)]_{u_i, v_i}$ is independent of $z, w \in \{-1, 1\}$. Since each b_i is oriented from u_i to v_i , we have that $[K_n]_{u_i, v_i} = c$, whence $J_I = c^{|I|}$.

Lemma 8.2. *Let A be a $2m \times 2m$ invertible, anti-symmetric matrix, and let $L \subseteq \{1, 2, \dots, 2m\}$ be a nonempty even subset. Let \widehat{A}_L be the submatrix of A obtained by deleting the rows and columns indexed by elements in L , and let A_L^{-1} be the submatrix of A^{-1} with rows and columns indexed by elements in L . Then*

$$(-1)^{S(L)} \text{Pf } \widehat{A}_L = \text{Pf}(A) \text{Pf}(A_L^{-1}), \quad \text{where } S(L) = \sum_{l \in L} l.$$

Proof. See the Appendix at Section 9. □

The conclusion of Lemma 8.2 holds also when $L = \emptyset$, subject to the convention that $\text{Pf}(A_\emptyset^{-1}) = 1$.

Returning to (8.5), take $L = \{|u_i|, |v_i| : i \in I\}$, so that $(-1)^{S(L)} = (-1)^{|I|}$. When the spectral curve does not intersect the unit torus \mathbb{T}^2 , by Lemma 8.2,

$$\begin{aligned} \lim_{n \rightarrow \infty} \frac{\text{Pf } \widehat{K}_{n,I}(z, w)}{\text{Pf } K_n(z, w)} &= \lim_{n \rightarrow \infty} (-1)^{|I|} \text{Pf } K_{n,I}^{-1}(z, w) \\ &= (-1)^{|I|} \text{Pf } K_I^{-1}, \end{aligned}$$

where the limit is independent of $z, w \in \{-1, 1\}$; see [19, Lemma 4.8] for a proof of the existence of the limits of the entries of K_n^{-1} . By (8.5)–(8.6),

$$(8.7) \quad \mu_\infty(M_I) = (-c)^{|I|} \text{Pf } K_I^{-1}.$$

We shall make use of the following elementary lemma, the proof of which is omitted.

Lemma 8.3. *Let S be a random subset of the finite nonempty set B . The probability generating function (pgf) $G(x) = \mathbb{E}(x^{|S|})$ satisfies*

$$G(1 + \lambda) = \sum_{I \subseteq B} \lambda^{|I|} \mathbb{P}(S \supseteq I), \quad \lambda \in \mathbb{R}.$$

Let B be the set of bisector edges along π (see (8.2)), and let S be the subset of such edges that are present in the dimer configuration. By (6.6),

$$\langle \sigma_e \sigma_f \rangle = G(-1),$$

where G is the pgf of $|S|$ under the measure μ_∞ . By (8.7) and Lemma 8.3,

$$(8.8) \quad \langle \sigma_e \sigma_f \rangle = \sum_{I \subseteq B} (-2)^{|I|} \mu_\infty(M_I) = \sum_{I \subseteq B} (2c)^{|I|} \text{Pf } K_I^{-1}.$$

This may be recognised as the Pfaffian of a certain matrix defined as follows.

Let $Y_1(\lambda)$ be the 2×2 matrix

$$Y_1(\lambda) = \begin{pmatrix} 0 & \lambda \\ -\lambda & 0 \end{pmatrix},$$

and let $Y_{2k}(\lambda)$ be the $4k \times 4k$ block diagonal matrix with diagonal 2×2 blocks equal to $Y_1(\lambda)$. More precisely, $Y_{2k}(\lambda)$ has rows and columns indexed $u_1, v_1, u_2, v_2, \dots, u_{2k}, v_{2k}$, and

$$Y_{2k}(\lambda) = \begin{pmatrix} Y_1(\lambda) & 0 & \cdots & 0 \\ 0 & Y_1(\lambda) & \cdots & 0 \\ \vdots & \vdots & \ddots & \vdots \\ 0 & 0 & \cdots & Y_1(\lambda) \end{pmatrix}.$$

Lemma 8.4. *We have that*

$$(8.9) \quad \langle \sigma_e \sigma_f \rangle = \text{Pf} [Y_{2k}(1) + 2cK_{V_\pi}^{-1}],$$

where $V_\pi = \{u_1, v_1, u_2, v_2, \dots, u_{2k}, v_{2k}\}$.

Proof. It suffices by (8.8) that

$$(8.10) \quad \text{Pf} [Y_{2k}(1) + A] = \sum_{I \subseteq B} \text{Pf } A_I,$$

where $A = (a_{i,j})$ is a $4k \times 4k$ anti-symmetric matrix with consecutive pairs of rows/columns indexed by the set $B = \{1, 2, \dots, 2k\}$, and A_I is the submatrix of A with pairs of rows and columns indexed by $I \subseteq B$.

Let $G = (V, E)$ be the complete graph with vertex-set $V = \{1, 2, \dots, 4k\}$, and recall (see [14, 26]) that

$$(8.11) \quad \text{Pf } A = \sum_{\mu \in \Pi} \text{sgn}(\pi_\mu) \prod_{\substack{(i,j) \in \mu \\ i < j}} a_{i,j},$$

where Π is the set of perfect matchings of G , and the permutation $\pi_\mu \in S_{4k}$ is given by

$$(8.12) \quad \pi_\mu = \begin{pmatrix} 1 & 2 & 3 & 4 & \cdots & 4k-1 & 4k \\ i_i & j_1 & i_2 & j_2 & \cdots & i_{2k} & j_{2k} \end{pmatrix}$$

where $\mu = \{(i_r, j_r) : 1 \leq r \leq 2k\}$, $i_1 < i_2 < \cdots < i_{2k}$, and $i_r < j_r$.

By (8.11),

$$(8.13) \quad \begin{aligned} \text{Pf } [Y_{2k}(1) + A] &= \sum_{\mu \in \Pi} \text{sgn}(\pi_\mu) \prod_{\substack{(i,j) \in \mu \\ i < j}} [Y_{2k}(1) + A]_{i,j} \\ &= \sum_{K \subseteq V} \left(\sum_{\mu \in \Pi} \text{sgn}(\pi_\mu) \prod_{\substack{(i,j) \in \mu \\ i \in K, i < j}} [Y_{2k}(1)]_{i,j} \prod_{\substack{(i,j) \in \mu \\ i \notin K, i < j}} a_{i,j} \right). \end{aligned}$$

The penultimate product is 0 unless every $i \in K$ is odd and satisfies $(i, i+1) \in \mu$. Therefore, with $J = \frac{1}{2}(K+1) \subseteq B$,

$$\begin{aligned} \text{Pf } [Y_{2k}(1) + A] &= \sum_{J \subseteq B} \left(\sum_{\mu \in \Pi} \text{sgn}(\pi_\mu) \prod_{\substack{(i,j) \in \mu, i < j \\ i, j \notin (2J-1) \cup (2J)}} a_{i,j} \right) \\ &= \sum_{J \subseteq B} \text{Pf } A_{B \setminus J}, \end{aligned}$$

as required for (8.10). □

Now, $Y_{2k}(1) + 2cK_{V_\pi}^{-1}$ is a truncated block Toeplitz matrix each block of which has size 4×4 . We propose to use Widom's formula (see Lemma 8.7) to study the limit of its determinant as $k \rightarrow \infty$. In this limit, the matrix becomes an infinite block Toeplitz matrix with symbol given by

$$(8.14) \quad \psi(z) = \frac{1}{2\pi} \int_0^{2\pi} \phi(z, e^{i\theta}) d\theta$$

where

$$(8.15) \quad \phi(z, e^{i\theta}) = Y_2(1) + 2cK_1^{-1}(z, e^{i\theta})_{(1:4)},$$

and $A_{(1:4)}$ denotes the 4×4 submatrix of the matrix A with rows and columns indexed by u_1, v_1, u_2, v_2 as in Figure 5.3. This follows by the explicit calculation

$$(8.16) \quad [K^{-1}]_{u,v} = \frac{1}{4\pi^2} \int_0^{2\pi} \int_0^{2\pi} e^{ik\phi} [K_1^{-1}(e^{i\theta}, e^{i\phi})]_{u,v'} d\theta d\phi, \quad u, v \in V_\pi,$$

where v' is the translation of v to the same fundamental domain as u , and k is the number of fundamental domains traversed in moving from v' to v , with sign depending on the direction of the move. When $k \neq 0$, (8.16) is the k th Fourier coefficient of the symbol (8.14). See [19, Sect. 4] for a similar computation.

Lemma 8.5. *Let $z \in \mathbb{C}$ with $|z| = 1$. When the spectral curve does not intersect the unit torus \mathbb{T}^2 , we have that $\det \psi(z) = 1$.*

Proof. Let $\mathbb{H}_{m,n,\Delta}$ be the toroidal graph comprising $m \times n$ fundamental domains (a fundamental domain is drawn in Figure 5.3). We can think of $\mathbb{H}_{m,n,\Delta}$ as the quotient graph of \mathbb{H}_Δ under the action of $m\mathbb{Z} \times n\mathbb{Z}$. To $\mathbb{H}_{m,n,\Delta}$ we allocate the clockwise-odd orientation of Figure 5.3.

Let $K_{m,n}(z, w)$ be the corresponding modified Kasteleyn matrix. Assume the cycle γ_x (respectively, γ_y) crosses $2n$ (respectively, $2m$) edges, whose weights are multiplied by z or z^{-1} (respectively, w or w^{-1}), depending on their orientations. Note that $K_{1,1} = K_1$.

The toroidal graph $\mathbb{H}_{1,n,\Delta}$ is a line of n copies of the graph of Figure 5.3, aligned parallel to γ_x . It contains $2n$ (bisector) edges with weight c , of which we select two, denoted e_1, e_2 , lying in the same fundamental domain. Let $\mathbb{H}_{1,n,\Delta}^*$ be the oriented graph obtained from $\mathbb{H}_{1,n,\Delta}$ by reversing the orientations of e_1 and e_2 , and let $K_{1,n}^*(z, w)$ be the modified Kasteleyn matrix of $\mathbb{H}_{1,n,\Delta}^*$.

Let $X(\lambda)$ be the $4n \times 4n$ matrix

$$X(\lambda) = \begin{pmatrix} Y_1(\lambda) & 0 & 0 \\ 0 & Y_1(\lambda) & 0 \\ 0 & 0 & 0 \end{pmatrix}.$$

Since e_1 and e_2 have weight c ,

$$\begin{aligned}
(8.17) \quad \frac{\det K_{1,n}^*(z, w)}{\det K_{1,n}(z, w)} &= \frac{\det[K_{1,n}^*(z, w) - K_{1,n}(z, w) + K_{1,n}(z, w)]}{\det K_{1,n}(z, w)} \\
&= \frac{\det[X(-2c) + K_{1,n}(z, w)]}{\det K_{1,n}(z, w)} \\
&= \det[X(-2c)K_{1,n}^{-1}(z, w) + I] \\
&= \det[Y_2(-2c)K_{1,n}^{-1}(z, w)_{(1:4)} + I] \\
&= \det[2cK_{1,n}^{-1}(z, w)_{(1:4)} + Y_2(1)],
\end{aligned}$$

for $w = \pm 1$, since $Y_2(1)Y_2(-1) = I$ and $\det Y_2(1) = 1$. Here, $K_{1,n}^{-1}(z, w)_{(1:4)}$ is the submatrix of $K_{1,n}^{-1}(z, w)$ comprising the rows and columns indexed by the four vertices incident with the e_i , see Figure 5.3.

By an explicit diagonalization of $K_{1,n}^{-1}$ as in [8, Sect. 7], for any two vertices u, v in the same fundamental domain, the limit

$$(8.18) \quad \lim_{n \rightarrow \infty} [K_{1,n}^{-1}(z, w)]_{u,v} = \frac{1}{2\pi} \int_0^{2\pi} [K_1^{-1}(z, e^{i\theta})]_{u,v} d\theta$$

exists and is independent of the choice of $w = \pm 1$. The proof of the next lemma is deferred until the current proof is completed.

Lemma 8.6. *For $z \in \mathbb{C}$, the limit*

$$(8.19) \quad \delta(z, w) = \lim_{n \rightarrow \infty} \frac{\det K_{1,n}^*(z, w)}{\det K_{1,n}(z, w)}$$

satisfies $\delta(z, -1) = \delta(z, 1) = \pm 1$.

We deduce that

$$\begin{aligned}
\det \psi(z) &= \lim_{n \rightarrow \infty} \det [Y_2(1) + 2cK_{1,n}^{-1}(z, 1)_{(1:4)}] \quad \text{by (8.14), (8.15), (8.18)} \\
&= \delta(z, 1) = \pm 1 \quad \text{by (8.17) and Lemma 8.6.}
\end{aligned}$$

Setting $z = 1$, we have by (8.19) that $\det \psi(1) \geq 0$ since it is the limit of a ratio of determinants of two anti-symmetric matrices. By (8.14) and the forthcoming (8.23), ψ is continuous on the unit circle when the spectral curve does not intersect \mathbb{T}^2 , and the claim follows. (Note that (8.23) is a general fact whose proof does not depend on Lemma 8.5.) Therefore, $\psi(z) = 1$ for $|z| = 1$. \square

Proof of Lemma 8.6. By (8.17)–(8.18), $\delta(z, -1) = \delta(z, 1) =: \delta(z)$, say. We claim that

$$(8.20) \quad \det K_{1,n}^*(z, -1) = \det K_{1,n}(z, 1), \quad \det K_{1,n}^*(z, 1) = \det K_{1,n}(z, -1).$$

By (8.19)–(8.20), $\delta(z, -1) = 1/\delta(z, 1)$, so that $\delta(z) = \pm 1$ as claimed.

We prove (8.20) next. Each non-vanishing term in the expansion of $\det K_{1,n}^*(z, -1)$ (respectively, $\det K_{1,n}(z, 1)$) corresponds to a cycle configuration on $\mathbb{H}_{1,n,\Delta}$, that is, a configuration of cycles and doubled edges in which each vertex has two incident edges. We may check, by an explicit consideration of the cases that can arise, that every corresponding pair of monomials in the two expansions have the same sign, and the first equation follows.

Here are some further details. Let C be an oriented cycle of $\mathbb{H}_{1,n,\Delta}^*$ viewed as an unoriented graph. It suffices that C contributes the same sign on both sides of (8.20). Let $c(C)$ (respectively, $w(C)$) be the number of c -type (respectively, w -type) edges crossed by C . By a consideration of parity, $c(C)$ is even if and only if $w(C)$ is even, and in this case C contributes the same sign. We claim that $w(C) = 1$ if $c(C) = 1$. It is standard that C is either contractible or essential, and that C , if essential, has homology type ± 1 in the direction γ_x . Therefore, $w(C) = 1$, and the claim follows. The second equation of (8.20) follows similarly. \square

We remind the reader of Widom’s theorem.

Theorem 8.7 (Widom [28, 29]). *Let $T_m(\psi)$ be a finite block Toeplitz matrix with given symbol ψ and $m \times m$ blocks. Assume*

$$\sum_{k=-\infty}^{\infty} \|\psi_k\| + \left(\sum_{k=-\infty}^{\infty} |k| \cdot \|\psi_k\|^2 \right)^{\frac{1}{2}} < \infty,$$

$$\det \psi(e^{i\theta}) \neq 0, \quad \frac{1}{2\pi} \Delta_{0 \leq \theta \leq 2\pi} \arg \det \psi(e^{i\theta}) = 0,$$

where $\|\cdot\|$ denotes Hilbert–Schmidt norm, ψ_k is the k th Fourier coefficient of ψ , and

$$\frac{1}{2\pi} \Delta_{0 \leq \theta \leq 2\pi} \arg \det \psi(e^{i\theta}) = \frac{1}{2\pi i} \int_{|\zeta|=1} d\zeta \frac{\partial}{\partial \zeta} \log \det \psi(\zeta).$$

Then

$$\lim_{m \rightarrow \infty} \frac{\det T_m(\psi)}{G(\psi)^{m+1}} = E(\psi),$$

where

$$(8.21) \quad G(\psi) = \exp \left\{ \frac{1}{2\pi} \int_0^{2\pi} \log \det \psi(e^{i\theta}) d\theta \right\},$$

$$(8.22) \quad E(\psi) = \det [T(\psi)T(\psi^{-1})],$$

and the last \det refers to the determinant defined for operators on Hilbert space differing from the identity by an operator of trace class.

Proof of Theorem 8.1. This holds as in the proofs of [19, Lemmas 4.4–4.7], and the full details are omitted. Here is an outline.

By (8.9) and Theorem 8.7, we may express $\Lambda(a, b, c)$ as the limiting determinant of a finite block Toeplitz matrix $T_m(\psi)$ with symbol $\psi(z)$ and $m \times m$ blocks. By Lemma 8.5, when the spectral curve does not intersect the unit torus \mathbb{T}^2 , we have $G(\psi) = 1$, where $G(\psi)$ is given in (8.21). Hence,

$$\Lambda(a, b, c) = \lim_{n \rightarrow \infty} \det T_n(\psi) = E(\psi),$$

where $E(\psi)$ is given in (8.22).

Non-analyticity of Λ may arise only as follows. One may write

$$(8.23) \quad [K_1^{-1}(z, w)]_{i,j} = \frac{Q_{i,j}(z, w)}{P(z, w)},$$

where $Q_{i,j}(z, w)$ is a Laurent polynomial in z, w derived in terms of certain cofactors of $K_1(z, w)$, and $P(z, w) = \det K_1(z, w)$ is the characteristic polynomial of the dimer model on $\mathbb{H}_{n,\Delta}$. It follows that Λ is analytic when $P(z, w)$ has no zeros on the unit torus \mathbb{T}^2 . The last occurs only under the condition of Proposition 5.1, and the claim follows. \square

9. APPENDIX: PROOF OF LEMMA 8.2

This proof makes use of an elementary lemma concerning monomials, of which the proof is omitted (see [18, p. 176, Cor. 1.6]). Let x_1, x_2, \dots, x_r be independent variables (which for concreteness we may take as real-valued). A *monomial* is a product of the form $\prod_{i=1}^r x_i^{n_i}$ where $n_i \in \{0, 1, 2, \dots\}$.

Lemma 9.1. *Let $(A_j : 1 \leq j \leq J)$ and $(B_k : 1 \leq k \leq K)$ be two sequences of distinct monomials. If*

$$(9.1) \quad \left| \sum_{j=1}^J \alpha_j A_j \right| \equiv \left| \sum_{k=1}^K \beta_k B_k \right|,$$

where $\alpha_j, \beta_k \in \mathbb{R} \setminus \{0\}$, then there exists $s \in \{-1, 1\}$ such that $(\alpha_j A_j)$ is a permutation of $(s\beta_k B_k)$.

Let $A = (a_{i,j})_{1 \leq i,j \leq 2m}$. By considering A^{-1} in terms of cofactors, we have that

$$(9.2) \quad \det \widehat{A}_L = \det(A) \det(A_L^{-1}),$$

see also [15, p. 601]. Since these matrices are anti-symmetric, they have Pfaffians which satisfy $\text{Pf } \widehat{A}_L = \pm \text{Pf}(A) \text{Pf}(A_L^{-1})$. We shall prove by induction on $\frac{1}{2}|L|$ that

$$(9.3) \quad \text{Pf } \widehat{A}_L = (-1)^{S(L)} \text{Pf}(A) \text{Pf}(A_L^{-1}).$$

Suppose first that $\frac{1}{2}|L| = 1$, and set $L = \{p, q\}$ with $1 \leq p < q \leq 2m$. Since $A_{\{p,q\}}^{-1}$ is a 2×2 anti-symmetric matrix,

$$(9.4) \quad \text{Pf}(A_{\{p,q\}}^{-1}) = [A^{-1}]_{p,q} = \frac{(-1)^{p+q} \det A^{q,p}}{\det A},$$

where $A^{q,p}$ is the $(2n-1) \times (2n-1)$ submatrix of A after deletion of the q th row and p th column. It suffices for (9.3) that

$$(9.5) \quad \det(A^{q,p}) = \text{Pf}(\widehat{A}_{\{p,q\}}) \text{Pf}(A),$$

and we have already by (9.2) and (9.4) that

$$(9.6) \quad |\det(A^{q,p})| = \left| \text{Pf}(\widehat{A}_{\{p,q\}}) \text{Pf}(A) \right|.$$

Lemma 9.2. *Equation (9.5) holds.*

Proof. We may assume without loss of generality that $p = 1, q = 2$. This is so by row/column movements as follows. If $p \neq 1$, the exchange of the columns labelled 1 and p (in addition to the corresponding row on the right side) changes the sign on both sides of (9.5). The same holds for row q (with column q on the right side).

Since each side of (9.5) is continuous in the $a_{i,j}$, we may assume for simplicity that $a_{i,j} \neq 0$ for $i \neq j$. Each term in (9.5) is a sum over monomials in the variables $\{a_{i,j} : i < j\}$, and (9.6) is an identity. By Lemma 9.1, the sets of monomials on the left and right sides of (9.5) are identical, and there exists $s \in \{-1, 1\}$ such that each monomial on the left of (9.4) appears also on the right with the coefficient s . It suffices to show that $s = 1$, and to this end it is enough to consider the sign of any single monomial.

We choose to consider the monomial

$$M = a_{1,2} [a_{3,4} a_{5,6} \cdots a_{2m-1,2m}]^2,$$

and we shall show, as required, that M has the same sign on the two sides of (9.5). Consider first the left side of (9.5), and recall for illustration that

$$(9.7) \quad \det A = \sum_{\sigma \in S_{2m}} \text{sgn}(\sigma) \prod_{i=1}^{2m} a_{i,\sigma(i)},$$

where S_{2m} is the set of permutations of $\{1, 2, \dots, 2m\}$. We replace A by $A^{2,1}$ in (9.7), and retain the labelling of rows and columns. The monomial M arises as the product of $m-1$ transpositions (r, s) , each of which contributes $a_{r,s} a_{s,r} = -a_{r,s}^2$. The ‘aggregate’ sign of M is $(-1)^{m-1} (-1)^{m-1} = 1$.

We turn to the right side of (9.5), and recall the definition (8.11) of $\text{Pf} A$ via matchings. The monomial M arises on the right side of (9.5) as the product $M =$

$M'M''$, where

$$M' = a_{3,4}a_{5,6} \cdots a_{2m-1,2m}, \quad M'' = a_{1,2}a_{3,4} \cdots a_{2m-1,2m}$$

contribute to $\text{Pf}(\widehat{A}_{\{1,2\}})$ and $\text{Pf}(A)$, respectively. By (8.12) or otherwise, the sign of M on the right side of (9.5) is $+$. The proof is complete. \square

We have proved (9.3) when $\frac{1}{2}|L| = 1$. We now prove it for general L by induction on $\frac{1}{2}|L|$. Here is the induction hypothesis:

$$H_l : (9.3) \text{ is true for } 1 \leq \frac{1}{2}|L| \leq l.$$

Let $k \geq 2$, and assume H_{k-1} holds.

Let $L = \{l_1, \dots, l_{2k}\}$, where $l_i < l_j$ if $i < j$. By expanding $\text{Pf} A_L^{-1}$ in terms of its first row,

$$\begin{aligned} (9.8) \quad \text{Pf}(A_L^{-1})\text{Pf}(A) &= \sum_{j=2}^{2k} (-1)^j [A^{-1}]_{l_1, l_j} \text{Pf}(A_{L \setminus \{l_1, l_j\}}^{-1}) \text{Pf}(A) \\ &= \sum_{j=2}^{2k} (-1)^j \text{Pf}(A_{L \setminus \{l_1, l_j\}}^{-1}) \left[\text{Pf}(A_{\{l_1, l_j\}}^{-1}) \text{Pf}(A) \right] \quad \text{by (9.4)} \\ &= \sum_{j=2}^{2k} (-1)^{j+l_1+l_j} \text{Pf}(A_{L \setminus \{l_1, l_j\}}^{-1}) \text{Pf}(\widehat{A}_{\{l_1, l_j\}}), \quad \text{by } H_1. \end{aligned}$$

By H_{k-1} , we have that

$$(9.9) \quad \text{Pf}(A_{L \setminus \{l_1, l_j\}}^{-1}) = (-1)^{S(L)-l_1-l_j} \frac{\text{Pf}(\widehat{A}_{L \setminus \{l_1, l_j\}})}{\text{Pf}(A)},$$

which we substitute into (9.8) to obtain

$$(9.10) \quad \text{Pf}(A_L^{-1})\text{Pf}(A) = (-1)^{S(L)} \sum_{j=2}^{2k} (-1)^j \frac{\text{Pf}(\widehat{A}_{L \setminus \{l_1, l_j\}}) \text{Pf}(\widehat{A}_{\{l_1, l_j\}})}{\text{Pf}(A)}.$$

Therefore, in order to prove H_k it suffices to prove that

$$(9.11) \quad \sum_{j=2}^{2k} (-1)^j \text{Pf}(\widehat{A}_{L \setminus \{l_1, l_j\}}) \text{Pf}(\widehat{A}_{\{l_1, l_j\}}) = \text{Pf}(A) \text{Pf}(\widehat{A}_L).$$

By (9.2), we have $|\text{Pf}(A_L^{-1})\text{Pf}(A)| = |\text{Pf}(\widehat{A}_L)|$, whence, by (9.10),

$$(9.12) \quad \left| \sum_{j=2}^{2k} (-1)^j \text{Pf}(\widehat{A}_{L \setminus \{l_1, l_j\}}) \text{Pf}(\widehat{A}_{\{l_1, l_j\}}) \right| = \left| \text{Pf}(A) \text{Pf}(\widehat{A}_L) \right|.$$

Lemma 9.3. *Equation (9.11) holds.*

Proof. As in the proof of Lemma 9.2, it suffices to prove that any given monomial appears on the left and right sides of (9.11) with the same sign. As before, we lose no generality by taking $L = \{1, 2, \dots, 2k\}$.

We choose to consider the monomial

$$M = a_{1,2} \cdots a_{2k-1,2k} a_{2k+1,2k+2}^2 \cdots a_{2m-1,2m}^2$$

on the right side of (9.11), comprising the product of $a_{1,2} a_{3,4} \cdots a_{2m-1,2m}$ from $\text{Pf}(A)$ and $a_{2k+1,2k+2} \cdots a_{2m-1,2m}$ from $\text{Pf}(\widehat{A}_L)$. The signs of the two corresponding permutations are $+1$, whence the corresponding sign of M is $+$. The corresponding monomial on the left side of (9.11) is

$$(-1)^2 [a_{3,4} \cdots a_{2m-1,2m}] \times [a_{1,2} a_{2k+1,2k+2} \cdots a_{2m-1,2m}],$$

where these two terms are taken from $\text{Pf}(\widehat{A}_{\{1,2\}})$ and $\text{Pf}(\widehat{A}_{L \setminus \{1,2\}})$, respectively. This product also has sign $+$, and equation (9.11) follows. \square

ACKNOWLEDGEMENT

This work was supported in part by the Engineering and Physical Sciences Research Council under grant EP/103372X/1. ZL acknowledges support from the Simons Foundation under grant #351813.

REFERENCES

- [1] M. Aizenman, D. J. Barsky, and R. Fernández, *The phase transition in a general class of Ising-type models is sharp*, J. Statist. Phys. **47** (1987), 342–374.
- [2] P. Billingsley, *Convergence of Probability Measures*, Wiley, New York, 1968.
- [3] M. Biskup, *Reflection positivity and phase transition in lattice spin models*, Methods of Contemporary Mathematical Statistical Physics, Springer, Berlin, 2009, pp. 1–86.
- [4] C. Boutillier and B. de Tilière, *The critical Z-invariant Ising model via dimers: the periodic case*, Probab. Theory Related Fields **147** (2010), 379–413.
- [5] ———, *Statistical mechanics on isoradial graphs*, Probability in Complex Physical Systems (J.-D. Deuschel, B. Gentz, W. König, M. von Renesse, M. Scheutzow, and U. Schmock, eds.), Springer Proceedings in Mathematics, vol. 11, 2012, pp. 491–512.
- [6] D. Chelkak and S. Smirnov, *Discrete complex analysis on isoradial graphs*, Adv. Math. **228** (2011), 1590–1630.
- [7] ———, *Universality in the 2D Ising model and conformal invariance of fermionic observables*, Invent. Math. **189** (2012), 515–580.
- [8] H. Cohn, R. Kenyon, and J. Propp, *A variational principle for domino tilings*, J. Amer. Math. Soc. **14** (2000), 297–346.
- [9] H. Duminil-Copin, R. Peled, W. Samotij, and Y. Spinka, *Exponential decay of loop lengths in the loop $O(n)$ model with large n* , (2014), to appear.
- [10] M. E. Fisher, *Statistical mechanics of dimers on a plane lattice*, Phys. Rev. **124** (1961), 1664–1672.

- [11] H.-O. Georgii, O. Häggström, and C. Maes, *The random geometry of equilibrium phases*, Phase Transitions and Critical Phenomena, vol. 18, Academic Press, San Diego, CA, 2001, pp. 1–142.
- [12] G. R. Grimmett, *The Random-Cluster Model*, Springer, Berlin, 2006, available at <http://www.statslab.cam.ac.uk/~grg/books/rcm.html>.
- [13] G. R. Grimmett and Z. Li, *Critical surface of a polygon model*, (2015), in preparation.
- [14] P. W. Kasteleyn, *The statistics of dimers on a lattice, I. The number of dimer arrangements on a quadratic lattice*, Physica **27** (1961), 1209–1225.
- [15] R. Kenyon, *Local statistics of lattice dimers*, Ann. Inst. H. Poincaré, Probab. Statist. **33** (1997), 591–618.
- [16] ———, *An introduction to the dimer model*, School and Conference on Probability Theory, ICTP Lect. Notes, XVII, Abdus Salam Int. Cent. Theoret. Phys., Trieste, 2004, pp. 267–304.
- [17] R. Kenyon, A. Okounkov, and S. Sheffield, *Dimers and amoebae*, Ann. Math. **163** (2006), 1019–1056.
- [18] S. Lang, *Algebra*, revised 3rd ed., Graduate Texts in Mathematics, vol. 211, Springer, New York, 2002.
- [19] Z. Li, *Critical temperature of periodic Ising models*, Commun. Math. Phys. **315** (2012), 337–381.
- [20] ———, *1-2 model, dimers and clusters*, Electron. J. Probab. **19** (2014), 1–28.
- [21] ———, *Spectral curves of periodic Fisher graphs*, J. Math. Phys. **55** (2014), Paper 123301, 25 pp.
- [22] ———, *Uniqueness of the infinite homogeneous cluster in the 1-2 model*, Electron. Commun. Probab. **19** (2014), 1–8.
- [23] C. Mercat, *Discrete Riemann surfaces and the Ising model*, Commun. Math. Phys. **218** (2001), 177–216.
- [24] M. Schwartz and J. Bruck, *Constrained codes as networks of relations*, IEEE Trans. Inform. Th. **54** (2008), 2179–2195.
- [25] H. N. V. Temperley and M. E. Fisher, *Dimer problem in statistical mechanics—an exact result*, Philos. Mag. **6** (1961), 1061–1063.
- [26] R. Thomas, *A survey of Pfaffian orientations of graphs*, Proceedings of the International Congress of Mathematicians, vol. III, Europ. Math. Soc., Zurich, 2006, pp. 963–984.
- [27] L. G. Valiant, *Holographic algorithms*, SIAM J. Comput. **37** (2008), 1565–1594.
- [28] H. Widom, *On the limit of block Toeplitz determinants*, Proc. Amer. Math. Soc. **50** (1975), 167–173.
- [29] ———, *Asymptotic behavior of block Toeplitz matrices and determinants. II*, Adv. Math. **21** (1976), 1–29.

STATISTICAL LABORATORY, CENTRE FOR MATHEMATICAL SCIENCES, CAMBRIDGE UNIVERSITY, WILBERFORCE ROAD, CAMBRIDGE CB3 0WB, UK

CURRENT ADDRESS (Z.L.): DEPARTMENT OF MATHEMATICS, UNIVERSITY OF CONNECTICUT, STORRS, CONNECTICUT 06269-3009, USA

E-mail address: g.r.grimmett@statslab.cam.ac.uk, zhongyang.li@uconn.edu

URL: <http://www.statslab.cam.ac.uk/~grg/>

URL: <http://www.math.uconn.edu/~zhongyang/>